Check for updates

Fluorine-containing macrocyclic peptides and peptidomimetics

Neshat Rozatian [iD] *[a,b] and Stefan Roesner [iD] *[a,c]

Fluorination plays a vital role in medicinal chemistry due to the unique properties of the fluorine atom. Macrocyclic peptides offer advantageous properties compared to linear peptides in drug discovery. In recent years, the development of fluorinated macrocyclic peptides and peptidomimetics, such as voxilaprevir, MK-0616 and ulimorelin, has highlighted the growing interest in the combination of fluorination and cyclization for tuning the properties of peptidic drug leads. In this review, the effects of fluorination on biological properties of macrocyclic peptides will be discussed. The use of the fluorine atom as a ^{19}F NMR spectroscopy probe for conformational studies of macrocyclic peptides will be reviewed. Finally, macrocyclic peptides containing the radionucleotide ^{18}F as PET imaging agents will be highlighted.

Introduction

Over the last 30 years, there has been continuously increasing interest in macrocyclic peptides. This is driven by their ability to improve many biophysical properties of peptides, such as binding affinity, specificity and proteolytic stability.[1,2] Macrocyclic peptides are predominantly peptidic structures bearing one or more rings containing multiple natural or non-natural amino acid residues. Examples include the antibiotic linopristin and the immunosuppressant cyclosporine. Of the more than 100 peptidic drugs that have reached the market, more than half are macrocyclic.[3,4] Cyclic peptides generally display improved pharmacokinetic and pharmacodynamic properties relative to their linear counterparts, making them promising leads in drug discovery.[5,6] Macrocyclization of peptides decreases the entropic cost of bonding, which can increase the affinity of peptides to their target.[7] A variety of

[a]*Department of Chemistry, University of Warwick, Gibbet Hill Road, Coventry, CV4 7AL, UK*

[b]*CatSci Ltd, CBTC2, Capital Business Park, Wentloog, Cardiff, CF3 2PX, UK. E-mail: neshat.rozatian@catsci.com*

[c]*School of Pharmacy and Biomolecular Sciences, Liverpool John Moores University, Byrom Street, Liverpool, L3 3AF, UK. E-mail: s.k.roesner@ljmu.ac.uk*

Neshat Rozatian

Neshat Rozatian received her PhD from Durham University in 2019, specializing in organofluorine and physical organic chemistries. She then joined the group of Prof. Michael Shipman at Warwick University as a Postdoctoral Research Fellow, working on azetidine-modified macrocyclic peptides. In 2023, she joined Iksuda Therapeutics, developing linker-payloads for incorporation into antibody–drug conjugates. She joined CatSci as a Senior Scientist in 2024, working within the process development team.

Stefan Roesner

Stefan Roesner completed his PhD at the University of Bristol, focusing on enantioselective lithiation–borylation reactions. He then moved to the US to undertake postdoctoral research at the Massachusetts Institute of Technology, working on palladium-catalyzed cross-coupling reactions under continuous-flow conditions. Following this, Stefan returned to the UK as a Senior Research Fellow and later Assistant Professor at the University of Warwick, collaborating with Prof. Michael Shipman on peptidomimetics and small nitrogen heterocycles. In April 2024, Stefan became a Senior Lecturer at Liverpool John Moores University, where he continues his research in organometallic and heterocyclic chemistry.

This journal is © the Partner Organisations 2025

Org. Chem. Front., 2025, **12**, 4871–4895 | **4871**

macrocyclization strategies have been developed over the years, including backbone cyclization, side-chain to side-chain cyclization, synthesis of lariat peptides, and many other methods, which have been reviewed elsewhere.[1,8–10] Macrocyclic peptides and peptidomimetics occupy a unique chemical space, and work has been done to define these regions according to Principal Component Analysis (PCA).[11] Non-peptidic macrocycles derived from amino acids with diverse applications have also been reviewed elsewhere.[12]

Fluorinated small molecules play a vital role in the pharmaceutical and agrochemical industries. 20% of drugs currently on the market contain fluorine and 50% of "blockbuster" drugs are fluorinated.[13] The introduction of fluorine into target molecules alters the pK_a, metabolic stability, binding affinities and other physicochemical properties, as well as conformational properties.[14,15] The unique properties of the C–F bond have enabled the tuning of macromolecule conformations through charge–dipole interactions, dipole–dipole interactions and hyperconjugation.[16] The fluorine atom can act as a bioisostere of the hydroxyl moiety, and the difluoromethyl moiety can function as a hydrogen bond donor. The effects of replacing alkoxy or hydroxy groups with a fluorine atom on lipophilicity ($\log P$) have been reported, whereby a structure-dependent increase in $\log P$ was generally observed.[17] The incorporation of fluorine into small molecule drugs can increase hydrophobicity, reduce metabolic degradation and initiate novel interactions with protein targets.[18] Synthetic methods of introducing a fluorine atom include electrophilic,[19] nucleophilic[20] and radical fluorination[21,22] as well as trifluoromethylation reagents.[23,24] Balz–Schiemann and Swarts halogen exchange processes are widely used for the production of fluoroaromatic and trifluoromethyl aromatic pharmaceuticals, respectively.[25] Over the last decade, numerous fluorine-containing building blocks have become commercially available, enabling *de novo* synthetic approaches.

The pharmaceuticals approved by the FDA between 2013 and 2024 included a number of fluorine-containing macrocyclic peptides, such as voxilaprevir, glecaprevir and motixafortide, which will be discussed in detail in this review.[26] Fluorine-containing peptides and proteins have increased enzymatic stability.[5] The effects of fluorine on conformations of side chains, folding kinetics and activity of linear peptides and proteins have discussed elsewhere.[27–29] Unnatural fluorinated amino acids are useful building blocks for the introduction of fluorine atoms into peptide structures.[30] The incorporation of fluoroaromatic linker groups provides an efficient macrocyclization strategy. In this review, we will discuss the strategies employed to alter the biological properties of macrocyclic peptides through fluorination. We will highlight examples where fluorine enabled the analysis of macrocycle conformation as well as the use of fluorine as a ^{19}F NMR reporter. Where relevant, we will include methods of fluorine incorporation into macrocyclic peptides. Ring sizes will be shown in blue at the center of structures. Finally, we will cover examples of macrocyclic peptides labeled with the radionucleotide ^{18}F for positron emission tomography (PET) imaging.

Altering biological properties using fluorine substitution

NS3/4A HCV protease inhibitors

Several fluorine-containing macrocyclic peptidomimetic drugs and lead compounds have been reported that target the hepatitis C virus (HCV) non-structural (NS) protein 3/4A protease. HCV causes chronic liver disease, cirrhosis, and hepatocellular carcinoma. Voxilaprevir (**1**, GS-9857), developed by Gilead Sciences, was the first fluorinated peptide drug on the market, approved in 2017 (Fig. 1a).[31] The key macrocyclic bond forming step involved ring-closing metathesis with Zhan 1b catalyst followed by reduction of the double bond. The difluoromethyl group at the P2 benzopyrazine resulted in improved genotype 3 potency through hydrophobic interactions between the difluoro group and R155, a resistance associated substitution (RAS) (Fig. 1a). A non-natural amino acid at P1 bears a further difluoromethyl group, which contributed toward improved metabolic stability.

Glecaprevir (**2**, ABT-493) is a next-generation, orally bioavailable drug for the treatment of HCV infections, developed by AbbVie and Enanta.[32] Marketed as Mavyret™, it is co-formulated with pibrentasvir (**3**), an NS5A inhibitor (Fig. 1b).[33] Sales of Mavyret™ reached $2.89 billion in 2019.[34] Glecaprevir contains four fluorine atoms as well as several amino acid moieties, including *tert*-Leu, Pro and ACC (1-aminocyclopropane-
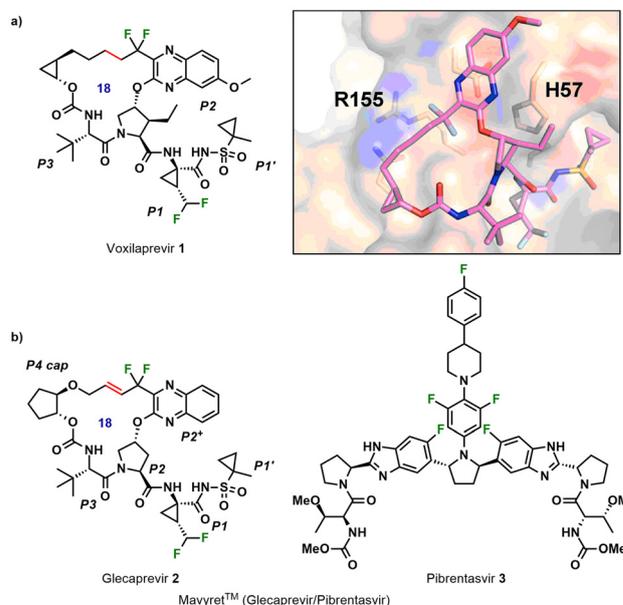

Fig. 1 (a) Structure of voxilaprevir **1** and its interaction in crystal structure bound to GT3 surrogate NS3/4A protease. Adapted with permission from ref. 31. Copyright 2019 Elsevier. (b) Structures of glecaprevir **2** and pibrentasvir **3**, marketed as Mavyret™, an HCV drug.

carboxylic acid). While structurally similar to voxilaprevir, glecaprevir's macrocycle contains an *E*-alkene, and the quinoxaline is unsubstituted at the C7-position. The medicinal route toward **2** comprised the synthesis of three key building blocks, including the preparation of the difluoromethylene containing quinoxaline derivative **7** (Scheme 1a) and the introduction of fluorine atoms using DAST to construct the difluorocyclopropylene moiety (Scheme 1b).[35] Macrocyclization was achieved by a ring-closing metathesis (RCM) reaction using a Ru catalyst (Scheme 1c). A scale up route to glecaprevir has also been reported.[36] Glecaprevir has *in vitro* EC$_{50}$ values in the low nanomolar range (0.85 to 2.8 nmol L^{-1}) across HCV genotypes 1–6.[37] In both voxilaprevir and glecaprevir, the difluoromethylene moiety is responsible for two orthogonal multipolar fluorine-specific interactions.[38] The highly electronegative fluorine atom promotes the formation of a caged fluorine-induced hydrogen bond between the hydrogen atom of the difluoromethyl moiety, the backbone carbonyl oxygen of the protease, and the carbonyl oxygen of the P1 group. Thus, the inhibitor is pre-organized for binding. Susceptibility to degradation is decreased through the incorporation of fluorine atoms in benzylic position within the macrocycle backbone. The resultant fluorine-specific interactions improve potency against all proteases genotypes.[39]

Resistance-associated substitutions (RAS) around the NS3/4A protease active site can affect the efficacy of antiviral agents by altering the shape and electrostatic properties of the S4 pocket. In the case of voxilaprevir (**1**) and glecaprevir (**2**), it has been shown that the fluorine atoms contribute toward the improved potency and antiviral activity across genotypes and resistant variants compared to the non-fluorinated HCV inhibitor grazoprevir (**13**, MK-5172, Fig. 2a).[31,40] To this end, a series of fluorinated analogs of **13** were synthesized, although the macrocycle was relocated from P2–P4 to P1–P3, to investigate the impact of modifications at the P2$^+$ quinoxaline moiety and the P4 capping group (Fig. 2b). The incorporation of fluorine near sites of RASs was found to improve antiviral activity
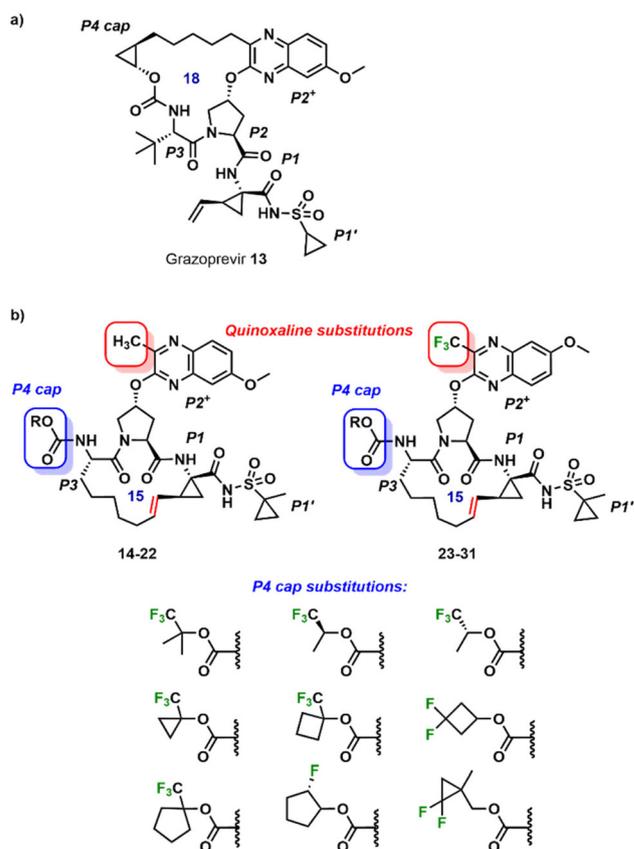

Fig. 2 (a) Structure of grazoprevir (**13**). (b) P1–P3 analogs of grazoprevir with quinoxaline and P4 cap substitutions.

across several HCV genotypes and resistance variants, due to its unique electronic properties and larger van der Waals radius.[41] Against the D168A protease variant, greater potency was retained in analogs fluorinated at P4 caps. Through analysis of co-crystal structures, it was revealed that fluorinated P4 caps could sample alternate binding conformations that enabled adaptation to structural changes induced by the D168A substitution.

Developed by Array BioPharma and InterMune Inc. and licensed to Roche, danoprevir (**32**) is a 15-membered macrocyclic peptidomimetic inhibitor of the NS3/4A HCV protease, containing a fluoroisoindoline (Fig. 3a).[42,43] This moiety lies in a lipophilic part of the protease's S2 pocket. Crystal structures have shown two equi-energetic conformations of danoprevir, with the fluorine atom either facing the P3 *tert*-butyl carbamate group or rotated 180° away from it (Fig. 3b). Danoprevir was identified as a clinical candidate due to its favorable potency profile against HCV genotypes 1–6 and key mutants, with IC$_{50}$ values between 0.2 and 0.4 nM. Clinical trials have recently been conducted to determine the effectiveness of danoprevir, in combination with ritonavir, against COVID-19.[44] Patients treated with danoprevir achieved negative nucleic acid test results in fewer days compared with those treated with other antivirals: an average time of 8 days to achieve a negative
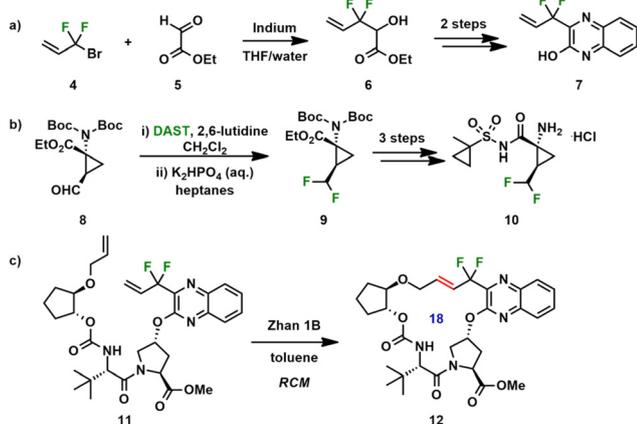
Scheme 1 (a) and (b) Synthesis of key fluorinated building blocks toward glecaprevir **2**. (c) Macrocyclization *via* RCM.

This journal is © the Partner Organisations 2025

Org. Chem. Front., 2025, **12**, 4871–4895 | **4873**

a)

Danoprevir **32**

c)

R = H   Simeprevir   **33**
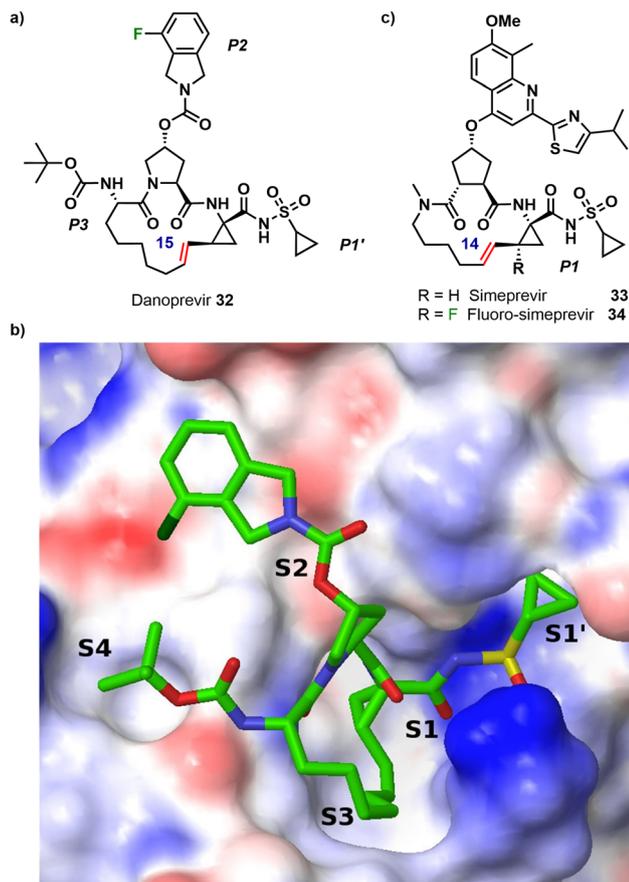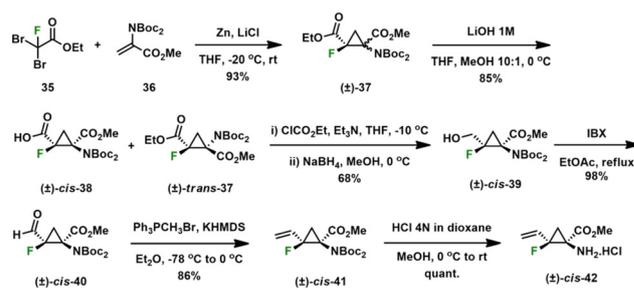R = F   Fluoro-simeprevir **34**

b)

Fig. 3 (a) Structure of danoprevir (**32**). (b) X-ray crystal structure of **32** bound to NS3 protease active site. Adapted with permission from ref. 42. Copyright 2013 American Chemical Society. (c) Structure of simeprevir (**33**) and its fluorinated analog **34**.

Scheme 2 Synthesis of fluorocyclopropane moiety **42**, a key structural component of fluoro–simeprevir **34**.

Paritaprevir **43**
1a-H77 EC$_{50}$ 1.0 nM
1b-con1 EC$_{50}$ 0.21 nM

diFluoro-paritaprevir **44**
1a-H77 EC$_{50}$ 2.0–5.0 nM
1b-con1 EC$_{50}$ 1.0–2.0 nM
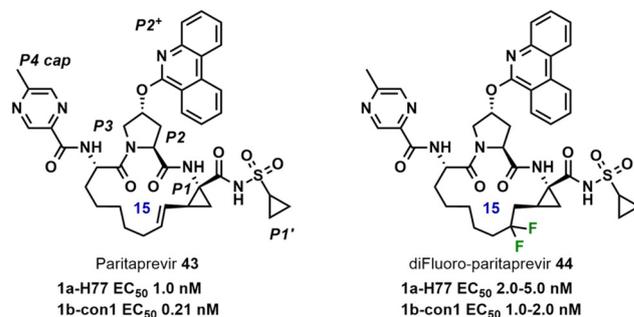
Fig. 4 Structures of paritaprevir **43** and CF$_2$-containing paritaprevir **44**.

test result compared with 12.5, and average hospital stay days of 11.4 compared with 16.7, were statistically significant.[45]

Simeprevir (**33**, TMC-435), a macrocyclic peptidomimetic, was developed by Janssen Pharmaceuticals Inc. and Medivir AB.[46] Milanole *et al.* reported the synthesis of a fluorinated analog of **33**, fluoro-simeprevir (**34**), a second-generation HCV NS3/4A serine protease inhibitor, containing a fluorocyclopropyl building block (Fig. 3c).[47] The synthesis of the unnatural amino acid is outlined in Scheme 2. In the fluorinated analog, the 1-amino-1-carboxyl-2-vinylcyclopropane core is essential for optimal fit in the hydrophobic S1 pocket of the NS3 protease. Installation of a single fluorine to the P1 cyclopropyl moiety in **33**, resulted in an 1800-fold increase in EC$_{50}$, from 8.1 nM to 15 μM. Modelling studies suggested some distortion in the P1–P2 conformation in which repulsion between the fluorine atom and the P2 carbonyl moiety led to a slight rotation that may also disturb the preferred orientation of the acylsulfonamide pharmacophore to the enzyme.

Fluorinated analogs of the peptidomimetic HCV NS3/4A protease inhibitor paritaprevir (**43**, ABT-450) have been reported (Fig. 4).[48,49] Analogs included variants with different heteroaryl substituents at P2$^+$ and the P4 cap, such as com-

pounds **48** and **53**. Two general strategies were used to incorporate the difluoromethylene moiety. Direct fluorination of the macrocycle **45** using the fluorinating reagent Morph-DAST (**46**) selectively converted a ketone into a difluoromethylene moiety (Scheme 3a). Alternatively, fluorine incorporation was achieved using unnatural amino acid **50** (Scheme 3b). Potencies of inhibition were measured against the HCV strains 1a-H77 and 1b-con1 and were reported to show low nanomolar EC$_{50}$ values.

BMS-986144 (**56**) is a pan-genotypic HCV NS3/4A protease inhibitor based on a P1–P3 macrocyclic tripeptide motif, developed as the next generation to the NS3 inhibitor asunaprevir (**54**) by Bristol Myers Squibb (BMS) (Fig. 5a and b).[50] Introduction of the P1–P3 macrocyclic tether to the structure of asunaprevir gave an 8-fold improvement in NS3/4A protease inhibitory potency, and selective functionalization of the tether with alkyl groups optimized both the enzyme inhibitory activity and the metabolic stability. An essential contributor toward higher stability was the trifluorinated Boc group, which addressed the issue of metabolism occurring at this moiety in asunaprevir.[51] Thus, the half-life in human liver microsomes (HLM) was increased from 6.4 min for macrocyclic asunaprevir (**55**) to 33 min for BMS-986144 (**56**). The isoquinoline moiety bearing a fluorine atom and a deuterated methoxy group (CD$_3$O) further improved the metabolic stability while preserving inhibitory potency.

MK-8831 (**58**) is a spiro-proline macrocycle developed by Merck as a pan-genotypic HCV NS3/4A protease inhibitor (Fig. 5c).[52] P1–P3 macrocyclization of the acyclic analog **57** improved the potency profile against several mutant variants

4874 | *Org. Chem. Front.*, 2025, **12**, 4871–4895

This journal is © the Partner Organisations 2025
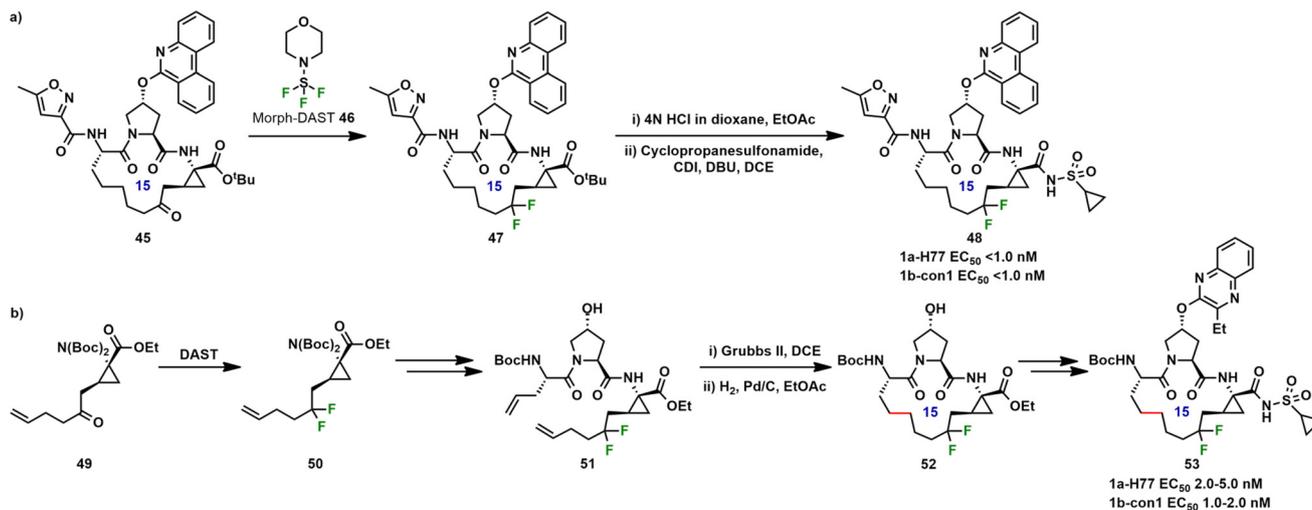
Scheme 3 (a) Fluorination of macrocycle **45** using Morph-DAST **46**. (b) Incorporation of CF$_2$-moiety into unnatural amino acid **49** and macrocyclization strategy.
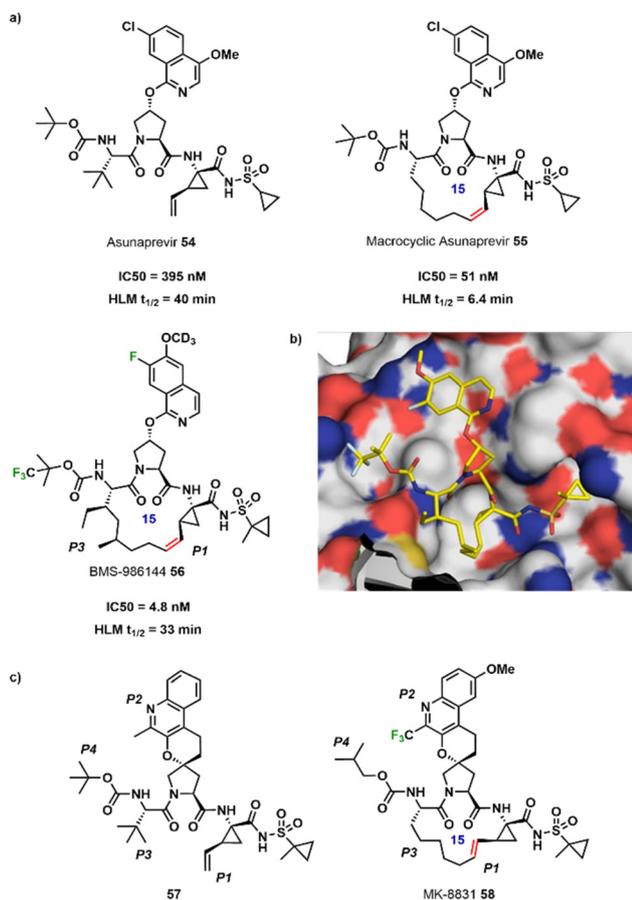

Fig. 5 (a) Structures of asunaprevir (**54**), macrocyclic analog **55**, and fluorinated macrocycle BMS-986144 (**56**); HLM = human liver microsomes. (b) Structure of **56** bound to GT-1a NS3/4A protease showing the surface of the enzyme. Adapted with permission from ref. 50. Copyright 2020 American Chemical Society. (c) MK-8831 (**58**) and its acyclic precursor **57**.

of genotype 1b, and with the introduction of a trifluoromethyl group to the quinoline, improved genotype 3a activity was also obtained. Following desirable pharmacokinetic profile and safety data, **58** was selected as a preclinical candidate and entered Phase 1 studies.

GS-9256 (**59**) is a HCV NS3/4A protease inhibitor reported by Gilead Sciences (Fig. 6a).[53] The macrocyclic structure features a phosphinic acid pharmacophore and a 2,6-difluorobenzyl group. In structure–activity relationship (SAR) studies, it was found that the 2,6-difluorobenzyl group modulated the low pK_a of the phosphinic acid group which was responsible for poor absorption of the non-fluorinated analog. The macrocyclic analogs were seven times more potent NS3 protease
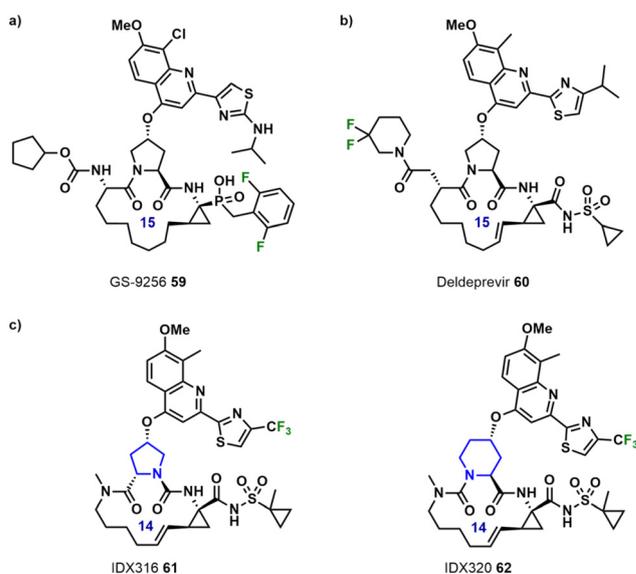

Fig. 6 Structures of (a) GS-9256 (**59**), (b) deldeprevir (**60**) and (c) IDX316 (**61**) and IDX320 (**62**).

This journal is © the Partner Organisations 2025

Org. Chem. Front., 2025, **12**, 4871–4895 | **4875**

inhibitors than non-macrocyclic derivatives. Following modification of the C-8 substituent with a chlorine atom which gave increased bioavailability, the compound with the best potency and pharmaceutical properties, GS-9256 (**59**), was selected for clinical trials. After a Phase IIb study, 95% of 42 patients treated with GS-9256 in combination with the antivirals tegobuvir, ribavirin and pegylated interferon achieved no detectable levels of HCV twelve weeks post-treatment.[54]

Deldeprevir (**60**) (neceprevir, ACH-2684) is a macrocyclic peptidomimetic inhibitor of NS3/4A protease containing a 3,3-difluoropiperidine moiety, developed by Achillion Pharmaceuticals (Fig. 6b).[55,56] In Phase Ib clinical trials, it was found to be well-tolerated and reduced the plasma HCV RNA levels in all groups. However, no further developments were reported since 2014.

The development route for the synthesis of macrocyclic trifluoromethylated thiazole structures IDX316 (**61**) and IDX320 (**62**) was reported by Idenix Pharmaceuticals Inc., including scale-up to half-kilogram cGMP batches of IDX320 (Fig. 6c).[57,58] Single- and multiple-dose studies on IDX320 demonstrated dose-dependent antiviral activity in HCV genotype 1 infected patients.[59] However, further development of IDX320 was halted due to the adverse occurrence of increased liver enzymes.

Examples for other therapeutic conditions

MK-0616 (**63**) is a macrocyclic peptide containing a fluoro-Trp moiety, developed by Merck for the treatment of hypercholesterolemia (Fig. 7).[60–62] **63** is currently in Phase III clinical trials as an oral inhibitor of proprotein convertase subtilisin/kexin type 9 (PCSK9).[63] Initially, a series of potent, orally bioavailable tricyclic PCSK9 inhibitors were reported, including compound **64**.[64] However, this was synthesized by an inefficient linear process and the sulfides were susceptible to oxidation. The redesigned structure **63** was synthesized through a convergent fragment-based strategy, where replacement of the thiol-based linker and central triazole reduced susceptibility to oxidation while maintaining high potency (**64** K_i = 2 pM *vs.* **63** K_i = 5 pM). **63** was found to inhibit PCSK9 in human plasma (IC$_{50}$ = 2.5 ± 0.1 nM), had low transcellular permeability, and no off-target activity in screening assays.

Fluorine-containing macrocyclic peptides have recently been identified for cancer treatment (Fig. 8). Motixafortide (**65**), sold under the name Aphexda™, has been approved for the treatment of pancreatic cancer and acute myeloid leukemia.[65] LUNA18 (**66**), reported by Chugai Pharmaceutical, is a highly bioavailable fluorinated macrocyclic peptide that acts as an inhibitor of Kirsten rat sarcoma viral oncogene homolog (KRAS), a common oncogene in numerous cancers.[66,67] The 4-CF$_3$-3,5-F$_2$-substituted aryl ring contributed toward improved PPI inhibitory activity, and LUNA18 showed significant efficacy against cancer cell lines with KRAS genetic alterations (IC$_{50}$ = 0.17–2.9 nM).

Ulimorelin (TZP-101, **67b**) is a macrocyclic peptidomimetic ghrelin receptor agonist, developed by Tranzyme Pharma as a first-in-class treatment for postoperative ileus and diabetic gas-

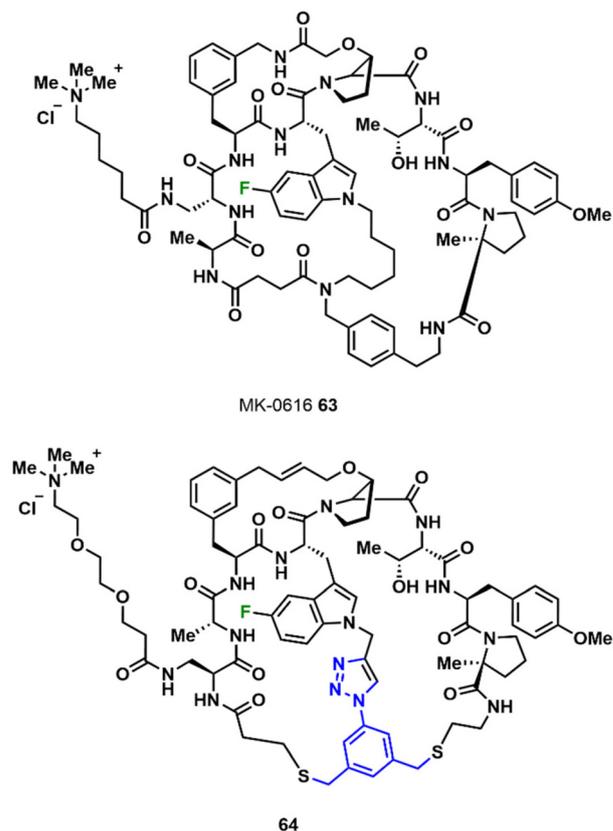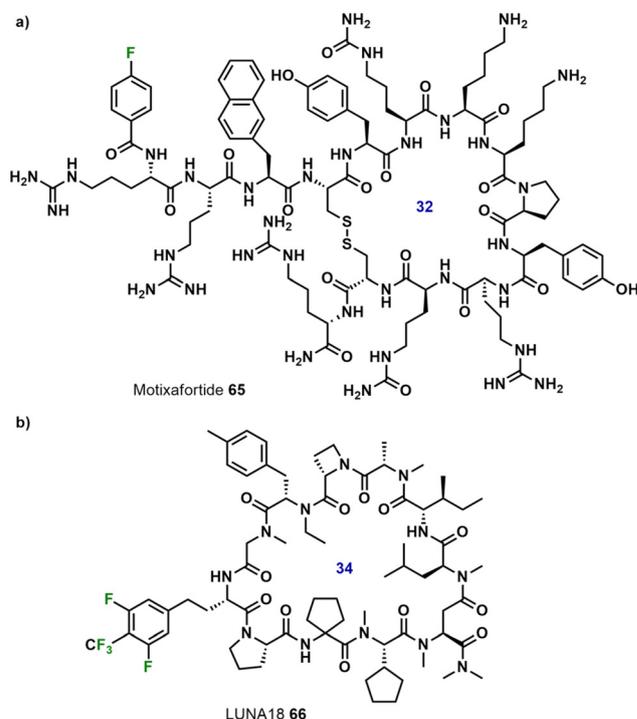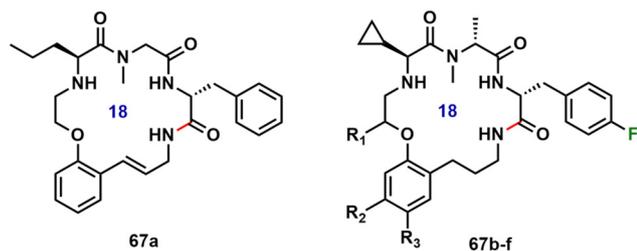**Fig. 7** Structure of MK-0616 (**63**) and related analog **64**.

Fig. 8 Structures of (a) motixafortide (**65**) and (b) LUNA18 (**66**).

4876 | *Org. Chem. Front.,* 2025, **12**, 4871–4895

This journal is © the Partner Organisations 2025

troparesis (Fig. 9).[68] Compound **67a** was initially identified as a lead GRLN agonist, and after further development, **67b** was selected as the clinical candidate. A key modification was the *para*-fluoro substituted Phe residue, the choice of which was supported by ligand lipophilicity efficiency (LLE) trends. SAR studies on the phenoxy ring substitution pattern showed a 2-fold improvement in binding potency, K_i, upon fluoro-substitution at the R_2 position compared to the unsubstituted derivative **67c**. On the other hand, R_3 fluoro-substitution in **67e** resulted in a 22-fold reduction in potency. PK profiling in rats highlighted desirable properties for **67b** and **67d**; however, PK profiling in monkeys revealed that the systemic clearance rate (CL) and absolute oral availability (%F) of ulimorelin (**67b**) were superior to those of **67d**, leading to its selection for clinical development.

MDL-104168 (**69**) is a macrocyclic human immunodeficiency (HIV) protease inhibitor containing a difluorostatone peptide mimetic, developed by Marion Merrell Dow (Fig. 10).[69] The original acyclic HIV-protease inhibitor, MDL-73669 (**68**), was cyclized *via* the P1 and P3 side chains, and the resulting macrocyclic peptide **69**, still retained good biological activity (K_i = 20 nM, IC_{50} = 2 nM). Such inhibitors are known to bind *via* the central hydrated difluorostatone by positioning the fluorine atoms within hydrogen bonding distance from catalytic aspartyl residue carboxylates, thus mimicking a key intermediate formed during the rate limiting step of normal hydrolysis of a substrate.[69]

A series of peptidic macrocycles bearing *N*-linked peptoid groups were developed targeting CXCR7, a chemokine receptor.[70] Building upon previously reported macrocyclic hexapeptide **70** with low nanomolar CXCR7 modulating activity,[71] significant structural alterations were made to improve the potency, selectivity and reduced off-target activity (Fig. 11). The potency was increased by addition of a 2,4-difluoro-substituted *N*-phenylpropyl side chain at the peptoid position. Peptide-peptoid hybrid **71** had the best overall balance between potency (K_i), polarity (EPSA) and passive permeability (P_{app}); therefore, it was progressed for *in vivo* oral absorption poten-
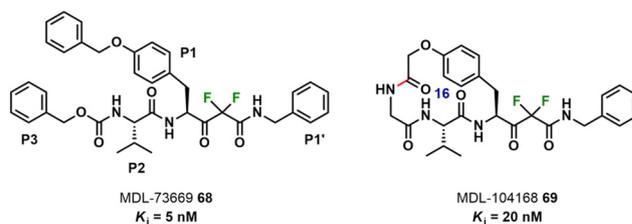

Fig. 10 Structures of linear (**68**) and macrocyclic (**69**) peptides containing a difluorostatone peptide mimetic.
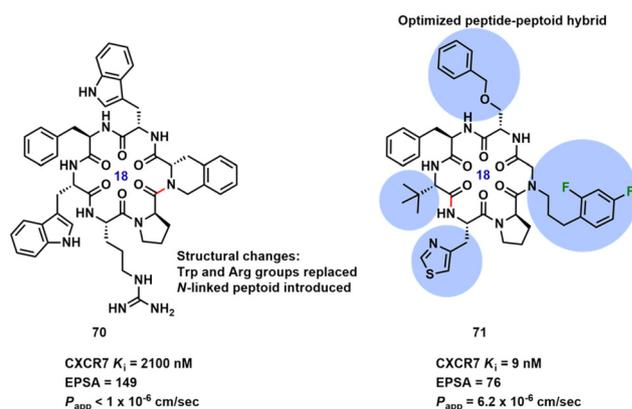

Fig. 11 Native macrocyclic hexapeptide structure **70** and structure of optimized peptide-peptoid hybrid **71**.

tial studies. A 3-fold improvement in the activity was obtained for **71** (EC_{50} = 15 nM) compared to the initial peptide **70** (EC_{50} = 46 nM).

A study reported that the binding affinity of a bicyclic FXIIa inhibitor **72** was enhanced ten-fold by replacing Phe with 4-fluorophenylalanine.[72] FXII is a serine protease involved in blood coagulation. A Trp was appended to the C-terminus of bicyclic peptide **72** for quantification by absorption spectrometry to determine K_i values shown in Fig. 12a. Fluorine substitution at the *ortho*-position reduced the activity approximately 2.5-fold. In contrast, *meta*- and *para*-substitution resulted in increased activities by 2- and 11-fold, respectively. The resulting peptide with 4-fluoro-Phe **72i** (without C-terminal Trp) had a K_i of 0.84 ± 0.03 nM. Structural modelling of the interactions between the bicyclic peptide and FXIIa showed that the side chain of the 4-fluoro-Phe residue was buried in an aromatic pocket formed by two surface loops (Fig. 12b). It was hypothesized that the short distance between the fluorine atom and both the polarized carbonyl and the α-hydrogen could result in polar interactions. In addition, the fluorine atoms could also perturb the electronic properties of the aromatic ring, thus enhancing the π–π stacking interactions between 4-fluoro-Phe and proximal His393 and Tyr439. Additional replacement of the terminal arginine residues by norarginine was found to increase the target selectivity 27 000-fold.

Flopristin (**73b**) is a semi-synthetic antibiotic of the streptogramin class (Fig. 13).[73,74] It is a fluorinated derivative of the

Fig. 9 Structure of ulimorelin (**67b**) and its analogs.

	Substitutions	K_i / nM	EC_{50}
67a	N/A	86	134
67b (Ulimorelin)	R_1 = (*R*)-Me, R_2 = R_3 = H	16	29
67c	none	7.3	ND
67d	R_2 = F, R_1 = R_3 = H	2.6	27
67e	R_3 = F, R_1 = R_2 = H	58	ND
67f	R_1 = (*R*)-Me, R_2 = F, R_3 = H	61	ND

This journal is © the Partner Organisations 2025

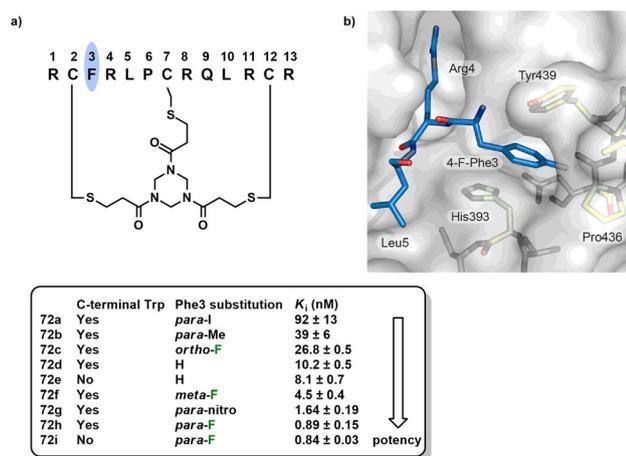*Org. Chem. Front.*, 2025, **12**, 4871–4895 | **4877**

Fig. 12 (a) Structures and activities of bicyclic FXIIa inhibitors **72a–i**. (b) Structural model for the three key amino acids 4-F-Phe3, Arg4 and Leu5 of bicyclic peptide **72i** bound to FXIIa. Adapted with permission from ref. 72. Copyright 2017 American Chemical Society.
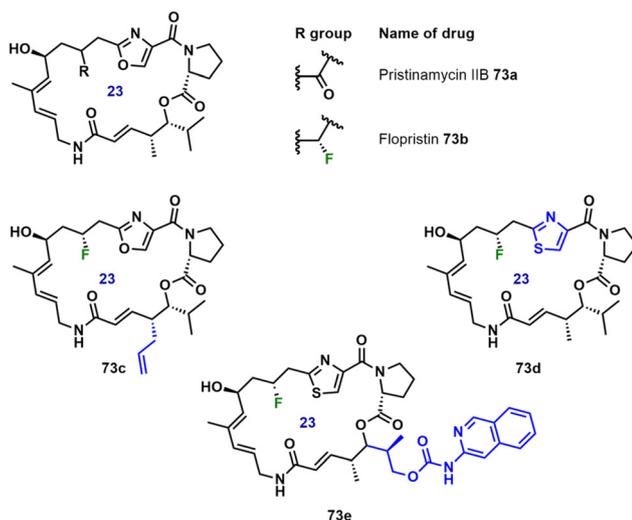

Fig. 13 Structures of pristinamycin IIB **73a** and flopristin **73b** and structures of flopristin analogs **73c–e**.

peptidic macrolactone pristinamycin IIB (**73a**, also known as virginiamycin M2) and is one of the components of the drug candidate NXL103, along with linopristin. Flopristin exhibited lower minimum inhibitory concentrations (MIC) than pristinamycin against *H. influenzae* and *H. parainfluenzae*.[73] NXL103 completed Phase II trials but no further progress has been reported. Analogs of flopristin containing the C16-fluoro group were described (**73c–e**), with the C4-allyl analog **73c** displaying up to a 128-fold improvement in MIC compared to the parent compound **73a**.[75] This compound had moderate activity (32 µg mL^{-1}) against ABC-F-expressing *E. faecalis* and Gram-negative *E. coli* (16 µg mL^{-1}), strains highly resistant to steptogramins. **73c** also showed greater activity compared to flopristin in multi-drug-resistant *S. aureus*. Furthermore, flopristin and

other fluorinated analogues were found to be more potent than the non-fluorinated lead compounds for inhibition of mitochondrial translation of glioblastoma stem cells. Higher cell membrane permeability was also demonstrated for the fluorinated macrocyclic peptides.[76]

Zhou *et al.* developed the macrocyclic peptidomimetic MCP-1 (**74f**, R = *meta*-di-F, Fig. 14), the most potent of a series of fluorinated analogs.[77] MCP-1 was found to bind to menin, an essential oncogenic cofactor for mixed lineage leukemia. Fluorine substituents at *ortho*, *meta* and *para* positions were introduced. Due to the acidic residues present along the phenyl binding site in the protein wall, it was proposed that the strong electronegativity of the fluorine atom could enhance polarization of the ring, leading to better binding affinities. *meta*-F substitution of MCP-1 gave a K_i value of 6.8 nM for binding to menin; hence, the molecule was 4-times more potent than the non-fluorinated derivative. Given the improved binding affinity to menin with F-substitution at the *meta* position, a new analog with two fluorine substituents at both *meta* positions was found to bind to menin with a K_i value of 4.7 nM, thus, showing a 6-fold improvement in potency compared to the non-fluorinated derivative. Macrocyclic MCP-1 was determined to be >600 times more potent than the corresponding linear peptide.

Tsunemi *et al.* reported macrocyclization through successive vinylic substitutions *via* reactions of octafluorocyclopentene (OFCP) with small peptides (Fig. 15) containing combinations of Cys, Tyr, His and Ser residues.[78] The macrocyclic peptidomimetics were stable upon storage, except Ser-linked **75a**, which underwent ring-opening over several weeks in deuterated DMSO solution. OFCP-linked macrobicyclic peptides such as **75e** were synthesized from the linear, unprotected precursors in polysubstitution cascades. Several of the OFCP-derived macrobicycles showed passive permeability in parallel artificial membrane permeability assays (PAMPA).[79]

Installation of a trifluoroacetyl (Tfa) moiety on the ε-amino group of lysine (K^{Tfa}) was found to be an effective method for the generation of peptide inhibitors of the human sirtuin (SIRT) family.[80] Of the three isoforms present, SIRT2 is involved in cell regulation by the deacetylation of ε-*N*-acetylated lysine residues (K^{Ac}) within α-tubulin and histone H4K16.[81] The macrocyclic structure of the peptide inhibitors, such as S2iL8 (**76**) shown in Fig. 16, led to a two-fold increase
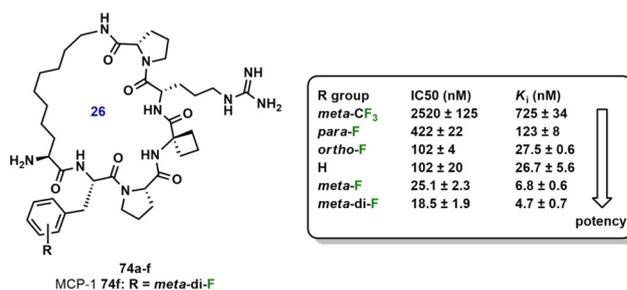

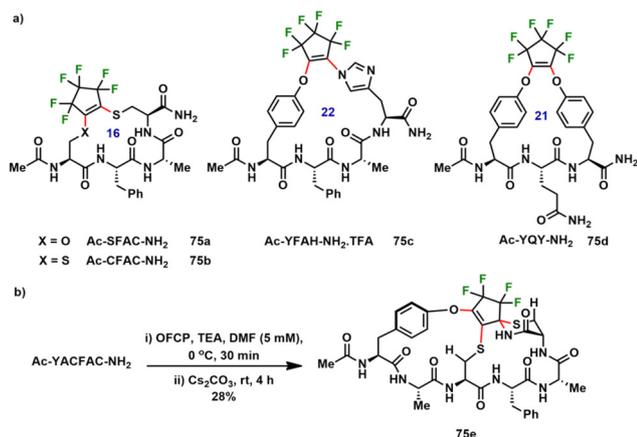**Fig. 14** MCP-1 (**74f**) and its analogs including their potencies.

4878 | *Org. Chem. Front.*, 2025, **12**, 4871–4895

This journal is © the Partner Organisations 2025

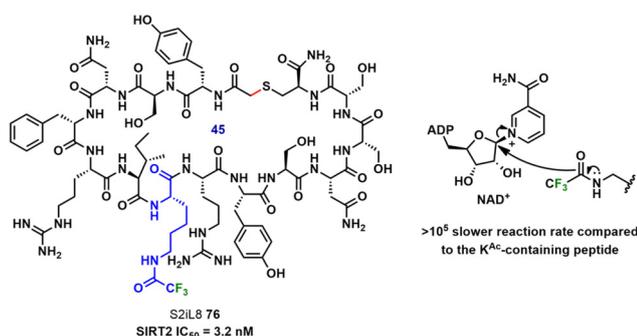**Fig. 15** (a) and (b) OFCP-derived macrocyclic peptides **75a–e**.

Fig. 16 Structure of the SIRT2-selective CF₃-containing macrocyclic peptide S2iL8 (**76**); the K^{Tfa} unit is highlighted.

Fig. 17 Structures of fluorine-containing cyclic pentapeptides **78a–l** based on the linear opioid peptide EM-2 (**77**).

in the inhibitory effect toward SIRT2 compared to linear analogs. Substitution of K^{Ac} with K^{Tfa} led to a slower reaction rate between the Tfa group and NAD$^+$, resulting in an unproductive intermediate and thus inhibition of sirtuin activity.

Fluorinated cyclic pentapeptide analogs of endomorphin-2 (EM-2, **77**) have been reported (Fig. 17).[82] Endomorphins are endogenous opioid neuropeptides that have attracted attention as pain relief drugs; however, linear EM peptides have suffered from poor receptor selectivity, rapid *in vivo* degradation, poor blood–brain barrier delivery and toxic side effects. Hence, the structure of EM-2 was modified by both cyclization and fluorination to improve biological activity. Twelve cyclic analogs **78a–l** were synthesized by individually replacing Phe residues with fluorinated amino acids (4-fluoro-Phe, 2,4-difluoro-Phe and 4-trifluoromethyl-Phe). Firstly, resistance toward *in vivo* enzymatic degradation was tested by incubating the cyclic pentapeptides with rat brain homogenate for 90 min and analyzing the amount of remaining peptide by RP-HPLC. **78a–l** all displayed less than 7% degradation, while EM-2 was almost completely digested. Next, pharmacological profiles of the analogs were investigated at three opioid receptors: μ-, δ- and κ-opioid peptides (MOP, DOP and KOP). Analogs containing mono- and di-fluorinated Phe residues were full MOP and

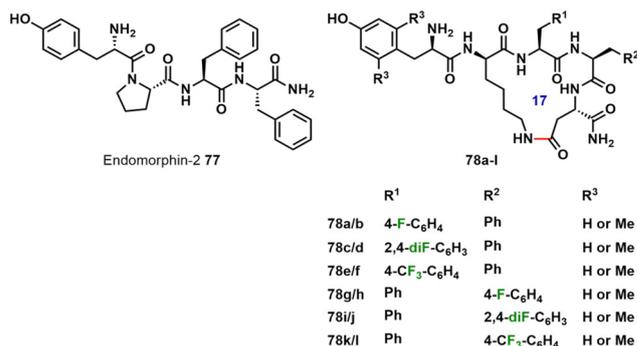partial KOP agonists, while showing lower potency and efficacy at the DOP receptor. Analogs containing 4-trifluoromethyl-Phe showed selectivity toward the KOP receptor. Finally, the most potent analogs, **78h** and **78j** produced a dose-dependent antinociceptive effect after both intracerebroventricular and intraperitoneal injection in mice, indicating that they were able to cross the blood–brain barrier.

The influence of a fluorine substituent was explored in a monocyclic analog of the trypsin inhibitor SFTI-1, in which the Lys5 in the substrate-specific P1 position of the wild-type SFTI-1 was replaced by 4-F-Phe to form analog **79** (Fig. 18).[83] The addition of the *para*-fluorine increased the inhibitory activity 15-fold compared to the non-fluorinated Phe analog. It was proposed that additional interactions of the *para*-substituent with chymotrypsin were responsible for the enhanced inhibitory activity of analog **79**. Furthermore, no significant difference in the chymotrypsin hydrolysis pattern was observed between analogs containing 4-F-Phe and Phe. Upon hydrolysis of the P1–P1′ bond, an equilibrium was reached between intact and hydrolyzed forms, where no further proteolysis was observed. This is notable due to the strict structural requirements for inhibitor-enzyme P1–P1′ interactions.
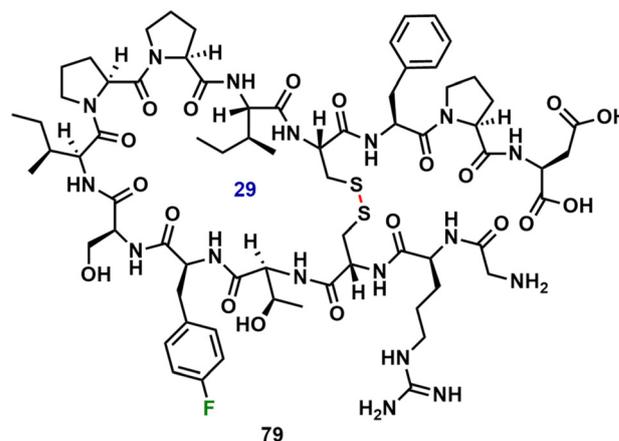

Fig. 18 Structure of **79**, a monocyclic analog of SFTI-1, a trypsin inhibitor.

This journal is © the Partner Organisations 2025

Org. Chem. Front., 2025, **12**, 4871–4895 | **4879**

The integration of the flexible *in vitro* translation (FIT) system into mRNA display technology resulted in the random non-standard peptide integrated discovery (RaPID) system, which has been used to discover *de novo* fluorinated macrocyclic peptides through ribosomal translation of fluorinated non-canonical amino acids (Fig. 19).[84,85] These macrocyclic peptides showed strong binding affinities for human ephrin type-A receptor 2 (EphA2), with K_D values of 9.9 nM (Ep-F1, **80a**) and 0.25 nM (Ep-F2, **80b**).[85] The fluorinated macrocyclic peptides were also found to disrupt the outer membrane of *E. coli*, resulting in lysis, as well as demonstrating broad-spectrum activity against multidrug-resistant Gram-negative bacteria by targeting the β-barrel assembly machinery (BAM) complex.

Another application of the RaPID and FIT systems was the incorporation of a Cys reactive electrophilic warhead, fluoroamidine, into macrocyclic peptide libraries.[86] Fluoroamidine is a small molecule inhibitor of peptidyl arginine deiminase 4 (PADI4), one of the enzymes that catalyze post-translational modification of peptidyl arginine residues to citrulline, which regulates cell signaling processes. Dysregulation of PADI4 is involved in diseases such as rheumatoid arthritis and lupus. In this report, an unnatural amino acid version of fluoroami-

dine, *N*-δ-fluoroacetimidoyl ornithine, was ribosomally incorporated into the peptide, such as the highly active cP4_4 (**81**, Fig. 20). It was found that the fluorine atom forms interactions within the PADI4 active site that are crucial for binding, as well as acting as the leaving group. The macrocyclic peptide itself ensured highly specific target binding and minimal off-target activity.

mRNA display technology was applied toward the *in vivo* selection of macrocyclic peptides containing unnatural amino acids, including macrocyclic peptide **82**, which bears a 3-fluoro-L-tyrosine and showed low nanomolar affinity for the protease thrombin (Fig. 21).[87,88] Following *in vitro* selection and evolution, the ribosomal synthesis of **82** was achieved *via* the cysteine residues and dibromoxylene. The macrocyclic nature of the peptides contributed significantly toward their affinity to thrombin, for example, a 25-fold decrease in K_d value was observed for inhibitor **82** compared to its linear counterpart.

A two-step combinatorial synthesis strategy was developed to synthesize a library of thioether-cyclized peptides, in which "*m*" random peptides were cyclized by "*n*" linkers followed by acylation at the peripheral amine with "*o*" carboxylic acids, to obtain "*m* × *n* × *o*" cyclic peptides (Scheme 4).[89] A number of fluorine-containing macrocyclic peptides were included in the library, although the specific effect of the fluorine atom was not investigated. A series of ten dithioether-linker macrocyclic peptides were incubated with liver microsomes and the metabolic stability was monitored by mass spectrometry. No correlation was found between oxidation rate and type of linker. A library of 8448 macrocyclic peptides was synthesized and screened against thrombin and, finally, multiple iterative cycles of library synthesis yielded peptides with oral bioavailability (%F) of up to 18% in rats.

Fluoroaromatic linker for the construction of macrocycles

The use of perfluoroaryl groups as reagents for peptide stapling through cysteine residues has been extensively investi-

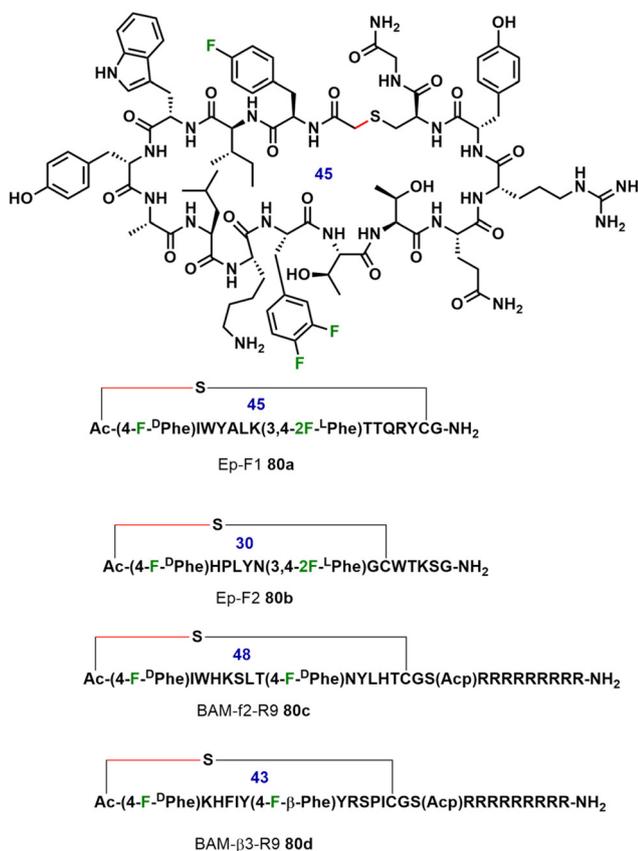**Fig. 19** Structures of *de novo* fluorinated macrocyclic peptides selected using the RaPID system targeting EphA2 (Ep-F1 **80a** and Ep-F2 **80b**) and Gram-negative pathogens (BAM-f2-R9 **80c** and BAM-β3-R9 **80d**). Acp = ε-aminocaproic acid.
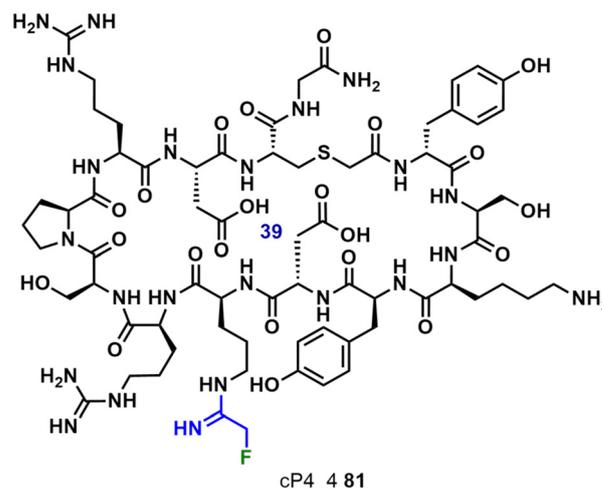

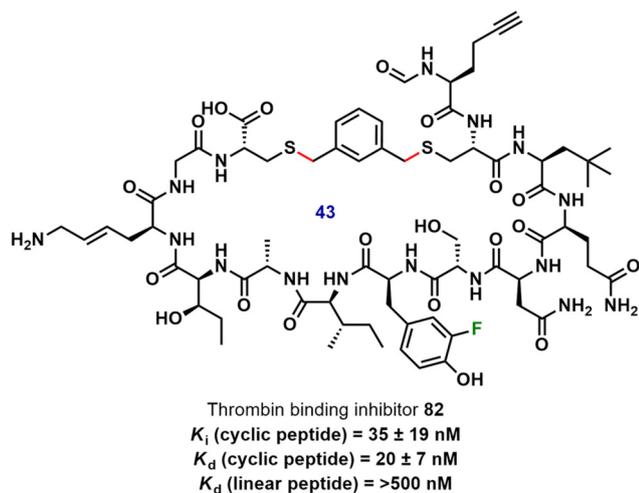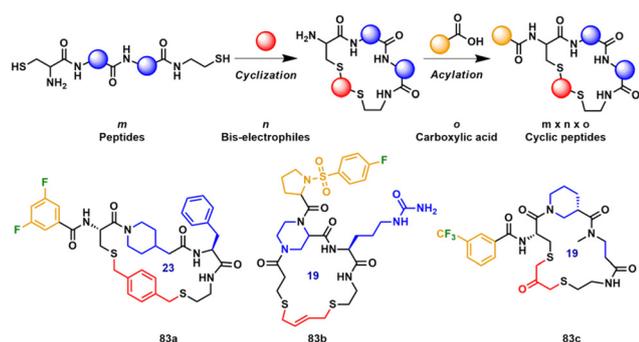**Fig. 20** Structure of fluoroamidine-containing macrocyclic peptide **81**.

4880 | *Org. Chem. Front.*, 2025, **12**, 4871–4895

This journal is © the Partner Organisations 2025

Thrombin binding inhibitor **82**
K_i (cyclic peptide) = 35 ± 19 nM
K_d (cyclic peptide) = 20 ± 7 nM
K_d (linear peptide) = >500 nM

Fig. 21 Structure of the thrombin inhibitor **82**.

Scheme 4 Combinatory synthesis of a library of thioether-cyclized peptides.

gated in recent years.[90,91] The field of perfluoroaryl reagents for peptide modification has been reviewed by Brittain and Coxon.[92] Perfluoroarylation can increase the lipophilicity of macrocyclic peptides as well as affecting their solubility and cellular penetration, however, the latter is also dependent on the physicochemical properties of the starting peptide.

Biocompatible macrocyclizations of peptides have been carried out using decafluoro-diphenylsulfone (DFS, **84**, Scheme 5).[93] Reaction rates for S_NAr at Cys residues with 12 different perfluoroarenes were measured *via* ^{19}F NMR spectroscopy in aqueous buffer, where reactions involving DFS were the fastest. The rates of macrocyclization correlated with the electronegativity of the substituents on the perfluoroarene ring. The rate enhancement was also attributed to the superior water solubility of DFS, compared to other perfluoroarenes such as hexafluorobenzene and perfluoronitrobenzene, which required an organic co-solvent. The reactivity of DFS was validated with model systems **85a–e**, with rate constants of up to 180 M^{-1} s^{-1}. DFS formed complex macrocyclic peptides of varying ring sizes, as demonstrated with six peptide-hormones: melanin-concentrating hormone **88** (MCH, Scheme 5), oxyto-
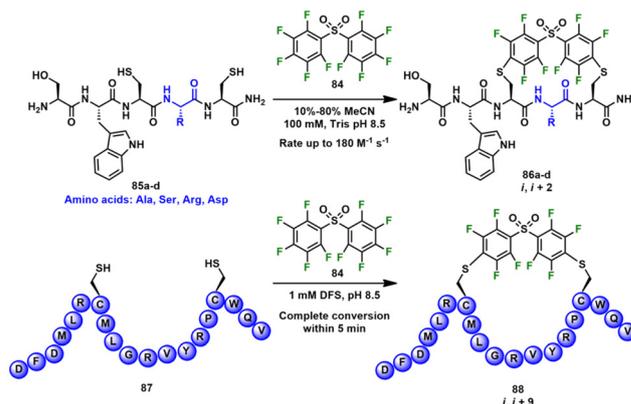
Scheme 5 Rapid biocompatible macrocyclization of peptides with DFS (**84**) between two cysteine residues.
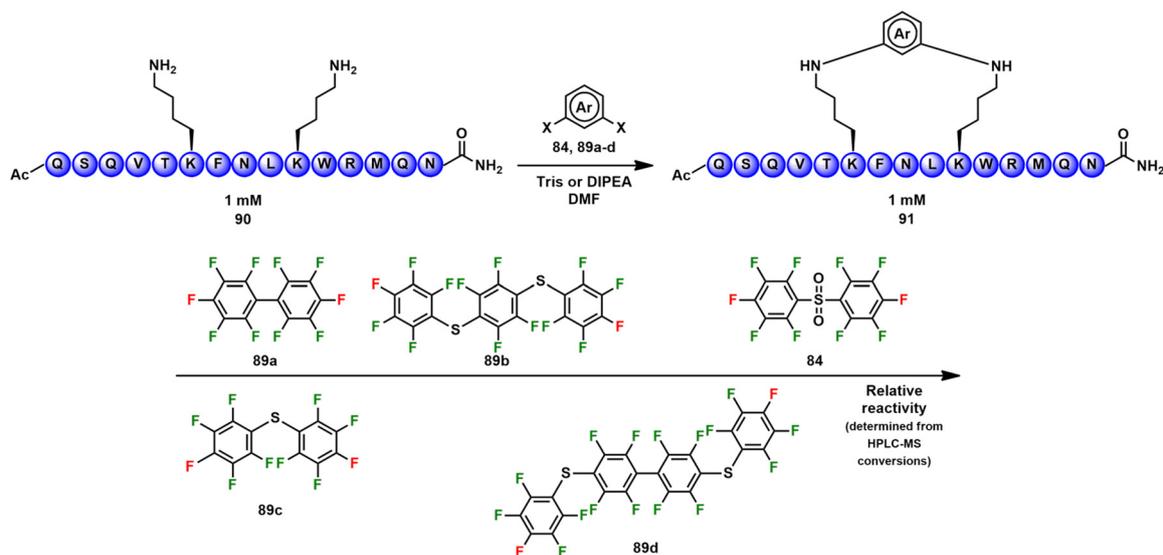
cin, urotensin II, salmon calcitonin, somatostatin-14, and atrial natriuretic factor (1–28), with ring sizes ranging from 6 to 19 amino acids. The rate of S_NAr was sequence dependent, with rate acceleration observed when positively charged Arg was present next to Cys. Conversely, negatively charged Asp reduced S_NAr rates. Advantages of the DFS framework over other perfluoroarene nucleophiles included biocompatibility with complex multiprotein complexes in aqueous solutions as demonstrated with bacteriophages, which otherwise would be degraded by organic solvents.

Independently to the previous report, Lautrette *et al.* reported the *N*-arylation of unprotected peptides using fluoroaromatic linker groups to synthesize stapled macrocyclic peptides.[94] The electrophilic linkers **84** and **89a–d** were ranked according to their relative reactivities with the unprotected linear peptide **90**, as determined by HPLC-MS analysis (Scheme 6). Oxidation of the perfluorosulfide to the perfluorosulfone resulted in a linker that was highly reactive, due to the promotion of the S_NAr by electron-withdrawing groups.

The "scanning approach" allows side-chain to side-chain macrocyclization irrespective of the sequence and position of the two amino acid residues.[95] A diversity-oriented synthetic (DOS) approach was taken to "scan" two cysteine residues positioned in sites ranging from *i*, *i* + 1 to *i*, *i* + 14 within 14 unprotected polypeptides.[96] Two complementary strategies were then developed for side-chain macrocyclization of the polypeptides. Cysteine cross-linking was performed either with perfluoroaryl-based linkers, or by first incorporating non-cross-linked perfluoroaryl-based moieties followed by macrocyclization with dithiol reagents. Using seven perfluoroaromatic linkers, 98 macrocyclic peptides were produced without the need for reaction optimization for each transformation.

Macrocyclization by perfluoroarylation has been shown to increase peptide stability and delivery of exon-skipping antisense oligonucleotides to cells.[97] Two strategies were reported for the synthesis of arginine-rich bicyclic peptides. The first bicyclization method involved trithiol moiety **92** to link three perfluoroaryl groups on the unprotected peptide chain **93** within 2 h and 62% isolated yield after HPLC purification

This journal is © the Partner Organisations 2025

Org. Chem. Front., 2025, **12**, 4871–4895 | **4881**

Scheme 6 *N*-Arylation of unprotected peptides and scale of reactivity for fluoroaromatic linker groups. Reactive fluorine atoms highlighted in red.

(Scheme 7a). In the second strategy, kinetically controlled bicyclization was carried out on the purified peptide **95** in DMF in the presence of DIPEA (Scheme 7b). This method took advantage of the slow rates of *i*, *i* + 1 cyclization previously observed with decafluorobiphenyl[96] and gave complete conversion to the *i*, *i* + 7 bicyclic peptide within 5 min. HPLC purification

gave the isolated bicycle **96** in 81% yield. The bicyclic peptide was then conjugated to phosphorodiamidate morpholino oligonucleotide (PMO) *via* a copper-catalyzed "click" reaction (Scheme 7c). PMOs are antisense oligonucleotides, such as eteplirsen, an FDA-approved therapy for the treatment of Duchenne muscular dystrophy (DMD).[98] The exon-skipping
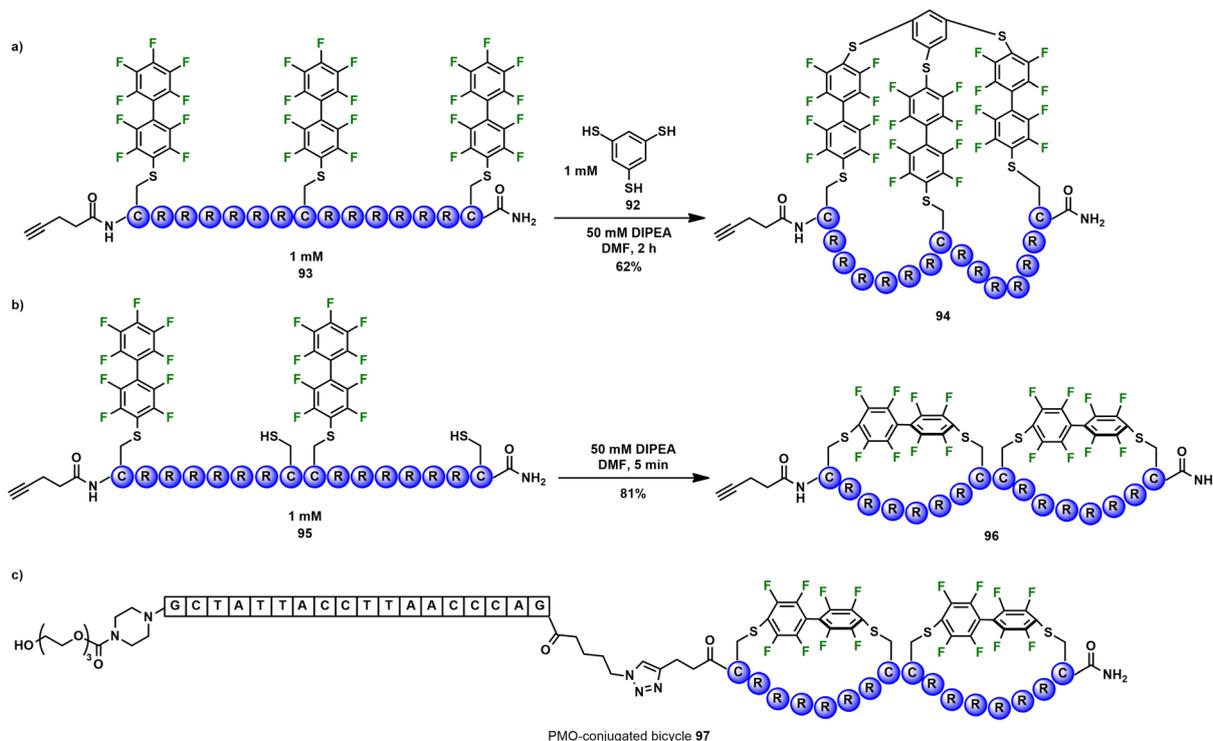
Scheme 7 (a) Peptide bicyclization *via* S$_N$Ar reactions of decafluorobiphenyl modified cysteine residues with 1,3,5-benzenetrithiol. (b) High-yielding kinetically controlled bicyclization *via* intramolecular S$_N$Ar at *i*, *i* + 7 positions. (c) Bicyclic peptide conjugated to phosphorodiamidate morpholino oligonucleotide (PMO).

4882 | *Org. Chem. Front.*, 2025, **12**, 4871–4895

This journal is © the Partner Organisations 2025
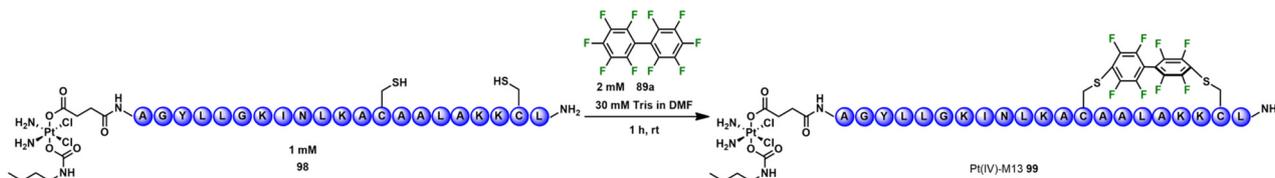
Scheme 8 Pt(IV)-prodrug peptide **98** cyclized *via* perfluoroaryl linker **89a**.

activity of the PMO-conjugated perfluoroaryl bicyclic peptide was greater than that of the non-fluorinated bicyclic peptide. Furthermore, the proteolytic stability of both bicycles **94** and **96** were greater than the corresponding *i*, *i* + 13 monocyclic peptide; after 1 h of incubation with trypsin, 70% of bicycle **94** and 45% of bicycle **96** remained undigested compared to only 5% of the monocyclic peptide.

Perfluoroaryl macrocyclic peptides were found to have greater penetration into brain endothelial cells, which, coupled with their increased serum stability, improved the delivery of small molecules across the blood–brain barrier.[99] This could improve the properties of new drugs for the treatment of brain tumors in diseases such as glioblastoma. Current cancer treatments include Pt(II) complexes, such as cisplatin, carboplatin and oxaliplatin, which have a narrow therapeutic index due to off-target toxicities.[100] A possible solution to widen the therapeutic index is administration as the Pt(IV) prodrugs, whereby, following cell internalization, the Pt(IV) prodrug is reduced *in situ* to the active Pt(II) species. To demonstrate improved delivery of Pt(IV) prodrugs across the blood–brain barrier, a Pt(IV) prodrug-perfluoroaryl macrocyclic peptide conjugate (Pt(IV)–M13, **99**) was synthesized (Scheme 8).[101] The peptide-prodrug conjugate **98** was prepared by coupling a Pt(IV) prodrug carboxylate to resin-bound peptide TP10 M13. A linear control conjugate, Pt(IV)–L13 conjugate, was also synthesized, in which Cys residues were replaced by Ser. The Pt(IV)–M13 conjugate **99**, Pt(IV)–L13 conjugate and cisplatin had IC$_{50}$ values of 4 μM, 29 μM and 2 μM, respectively.

Fluorine atom as a ^{19}F NMR reporter and a tool for conformational analysis of macrocyclic peptides

Fluorine-containing analogs **100a–f** of the cyclic decapeptide gramicidin S (GS) were developed by Wadhwani *et al.* (Fig. 22).[102] The highly NMR sensitive ^{19}F-reporter was attached to the GS backbone, through which the structure and dynamics of GS in its biologically relevant membrane-bound state were studied using solid-state ^{19}F and ^{15}N NMR spectroscopy.[103] The antimicrobial properties of GS were attributed to its destabilizing effect on lipid membranes. The alignment of the peptide in the bilayer and its temperature-dependent mobility were determined by analyzing the anisotropic chemical shift of the ^{19}F-labels in macroscopically oriented membranes. A narrowing of the ^{19}F NMR chemical shift dispersion was observed upon raising the temperature to the liquid crystalline state, due to the onset of global rotation of the peptide.
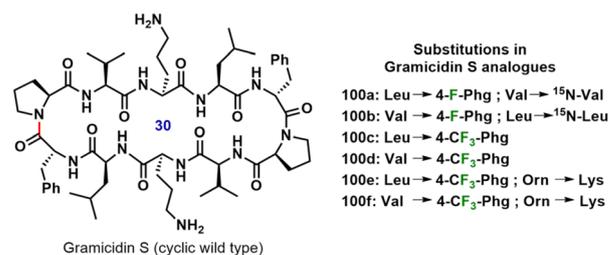
Fig. 22 Gramicidin S analogs **100a–f** functionalized with ^{15}N and ^{19}F NMR reporter groups.

It was proposed that the information elucidated from this study could be used to develop an analog more selective toward bacterial membranes.

Iterative conjugate addition/ring expansion (CARE) reactions were reported for the synthesis of macrocyclic peptide mimetics based on β-peptoid linkages.[104] *N*-Acylation of δ-valerolactam **101** with acryloyl chloride followed by CARE with *p*-fluorobenzylamine **102** afforded the 10-membered bis-lactam **103** (Scheme 9). The *p*-fluorobenzylamine **102** provided a convenient handle for reaction monitoring using ^{19}F NMR spectroscopy. A further *N*-acylation/CARE sequence was performed on **103** using three different amines (shown in blue) to
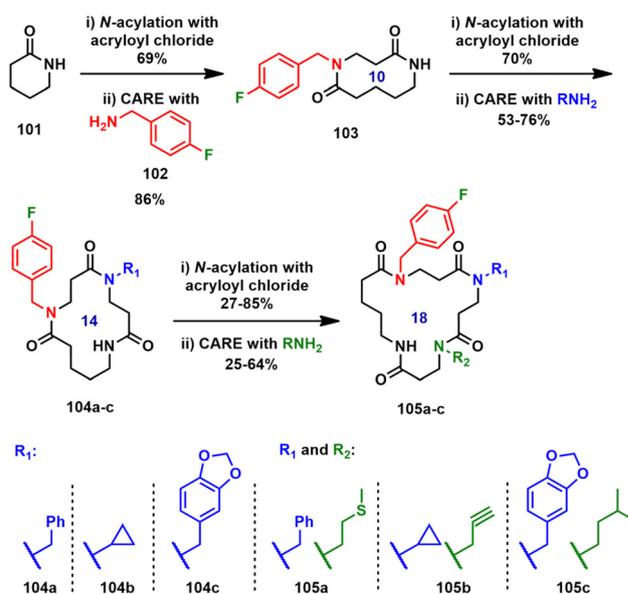
Scheme 9 Iterative *N*-acylation and CARE reactions.

This journal is © the Partner Organisations 2025

Org. Chem. Front., 2025, **12**, 4871–4895 | **4883**

synthesize 14-membered macrocycles **104a–c**. Compounds **104a–c** were iteratively expanded using different amines (shown in green) to afford 18-membered β-peptoid-derived tetrapeptide mimetics **105a–c**. A limitation of the CARE methodology is that it can only promote 4-atom ring expansions, hence, cyclic peptides with proteinogenic amino acids cannot be targeted.

To extend the *in vivo* circulation half-life of peptide therapeutics, a phage-displayed library was reported consisting of albumin-binding macrocyclic peptides modified with decafluoro-diphenylsulfone (DFS, **84**) to afford octafluoro-diphenyl-sulfone-cross-linked macrocycles **106** (Fig. 23).[105] Non-specific reactivity of OFS-macrocyclic peptides was observed with thiol nucleophiles, such as glutathione, at basic pH. Hence, the DFS was replaced with the less reactive pentafluorophenyl sulfide, to afford perfluorophenylsulfide (PFS) macrocycles which were unreactive toward free thiol on human serum albumin (HSA). The fluorine handle in the perfluoroaryl macrocyclic peptides allowed the determination of binding constants using ^{19}F NMR spectroscopy, whereby the broadening and disappearance of ^{19}F signals corresponding to fluoroaromatic groups indicated the binding of the macrocyclic peptide to HSA. The measured K_D values indicated that both the amino acid sequence and the perfluoroaromatic linker could affect binding. The main function of the perfluoroaromatic linchpin was to constrain the macrocyclic peptide in a productive albumin-binding conformation. The half-lives of PFS-SICRFFCGGG **107** and its analogs were evaluated in mouse plasma, where the concentration of the former was constant after 60 min, while the latter were rapidly cleared. Replacement of the PFS linker with hexafluorobenzene (HFB) and decafluorobiphenyl (DFB) reduced the concentration of the resulting macrocyclic peptides in plasma 10-fold compared to macrocycle **107**. This highlights that both the amino acid sequence and the albumin-binding conformational constraints imposed by the PFS linker are crucial for short-term retention in circulation.

The C–F bond as a conformational tool within peptides and proteins has been utilized to examine the α-fluoroamide effect and the F–C–C–N *gauche* effect.[106] Stereoselective fluorination has been demonstrated to alter the geometry of cyclic peptides. For their investigations, Hu *et al.* chose the marine-derived natural product, unguisin A, a cyclic heptapeptide bearing a γ-aminobutyric acid (GABA) residue (**109a**, Scheme 10).[107] The difluorinated amino acids **108a** and **108b**
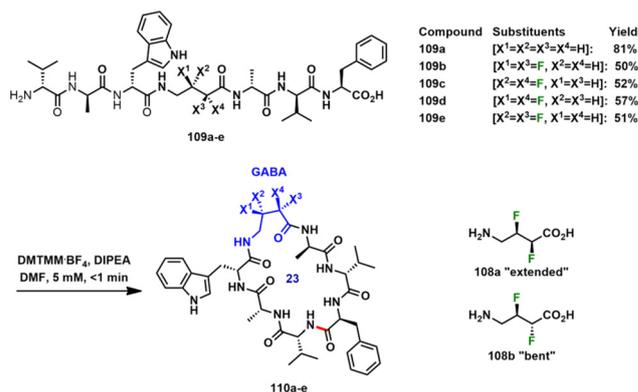
Scheme 10 Structure of unguisin A (**109a**) and its fluorinated analogs **109b–e**.

have been shown to introduce different selectivity patterns in GABA binding assays.[108] By replacing the GABA unit with either **108a** or **108b** or their enantiomers, analogs **110b–e** were synthesized in 50–57% yield. Monitoring the macrocyclization by ^{1}H NMR spectroscopy at 0 °C showed completion of the reactions within one minute. To understand the effects of fluorination on the secondary structure, $^3J_{HH}$, $^3J_{HF}$ and $^4J_{HF}$ values were determined. For isomers **110b–e**, the fluorine atoms were *gauche* but exhibited *g+/g−* disorder. Furthermore, energy minimizations showed that these fluoro-analogs displayed different geometries from that of **110a**. While **110a** was flat with a puckered seven-membered H-bonded ring (γ-turn), the *syn*-difluoro isomer **110b** displayed a planar geometry with no H-bonded turns. The other *syn*-difluoro isomer **110c** contained two overlapping H-bonded loops, an equatorial γ-turn and a distorted α-turn (a 13-membered H-bonded ring). **110d** and **110e** were both highly puckered, with a γ-turn and two β-turns (ten-membered H-bonded rings). Moreover, the role of flexibility in supramolecular interactions of unguisin A was studied using fluorine-containing macrocyclic peptides **110b–e** containing the GABA flexible spacer.[109] Fluorine substitution in molecules **110b–e** rigidified the structure and resulted in a 15–50% lower affinity toward chloride anions compared to unguisin A (**110a**). Finally, molecular dynamics (MD) simulations found that the difluorinated derivatives of unguisin A were flexible in DMSO solution which, depending on the fluorination pattern, adopted two or more conformations.[110]

Extending upon this work, a series of cyclic RGD tetrapeptides containing the fluorine-modified GABA moiety were reported to determine the effect of fluorine pattern on cyclization rates, as well as to assess the ability to tune molecular conformations and biological activities.[111] Both enthalpic and entropic contributions of the fluorinated segments were found to be significant for cyclization efficiencies. MD simulations showed substantial variation in conformations of the cyclic tetrapeptides, confirming that fluorination can alter secondary structures. Proof-of-concept studies on cell adhesion and cell spreading were performed, where significant differences were obtained depending on the position of fluorination.
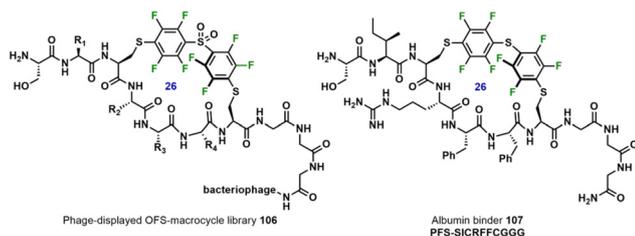

Fig. 23 Peptides modified with DFS and PFS linkers.

4884 | *Org. Chem. Front.*, 2025, **12**, 4871–4895

This journal is © the Partner Organisations 2025

Burade *et al.* reported the role of fluorine as a reverse turn inducer in acyclic αγα tripeptides containing fluorinated furanoid groups, which have potential applications as anion channels through antiparallel self-assembly of U-shaped monomers.[112] This work was extended to the synthesis of fluorinated sugar amino acid derived αγ-cyclic tetra- and hexapeptides. Macrocyclization was achieved using 2-chloro-1-methyl pyridinium iodide (CMPI) and *N,N*-diisopropylethylamine (DIPEA) in acetonitrile to afford α,γ-cyclic tetrapeptide **112** and α,γ-cyclic hexapeptide **114** (Scheme 11). Observed $^4J_{H,F}$ values of 2.2–3.1 Hz in macrocycles **112** and **114** suggested *gauche* conformation between C–F and N–H groups, resulting in antiparallel alignments of C–F and adjacent amide C=O bonds. The F–C–C=O torsion angle of 172.28° and dipole repulsion further supported this alignment, leading to weak intramolecular fluorine-amine hydrogen bonding interactions. These interactions led to the folding of cyclic peptides **112** and **114** into β-strand structures, and further self-assembly into nanotubes in both solution and gas phase. The nanotubes formed by **114** were shown to facilitate anion-selective transport of nitrate ions.

Cogswell *et al.* reported the synthesis of a macrocyclic peptide containing an α-fluoroalkoxyaryl group ArOCF$_2$R, which has the potential to function as a tool for studying conformational properties (Scheme 12).[113] A difluoroallylated tyrosine served as a building block to synthesize linear peptide **115** in three steps. Following hydrogenation to remove both Cbz and benzyl protecting groups, a macrolactamization reaction was performed to obtain the difluorinated macrocycle **116** in 64% yield. The ArOCF$_2$R group has been shown to reduce in-plane conformational preferences through hyperconjugation effects between low energy σ*C–F antibonding orbitals and oxygen lone pairs.[18,114] Although not investigated further in the report by Cogswell *et al.*, it was noted that macrocyclic peptides such as **116** could be used to study the impact of the ArOCF$_2$R group on conformational and physiochemical properties.

Numerous tryptophan-derived natural products contain the pyrroloindoline motif. Rose *et al.* reported a synthetic method
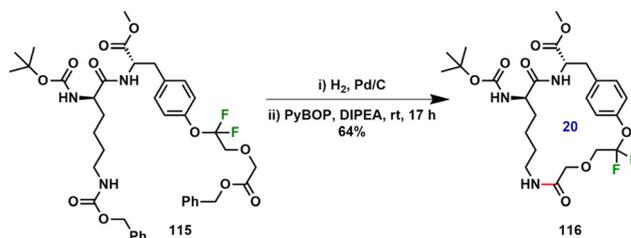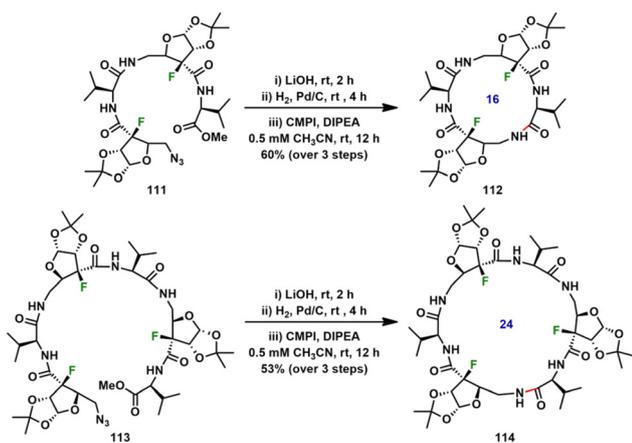
Scheme 12 Synthesis of a tyrosine-based difluoromethylene-containing macrocyclic peptide **116**.

where the indole activation step was, itself, the macrocyclization reaction.[115] Substrates bearing 5-methyl- and 5-fluoro-L-tryptophan (**117–118**, Scheme 13a) were synthesized in order to block previously observed pathways of C5 alkylation and, instead, to favor macrocyclization *via* electrophilic substitution at indole C3.[115,116] In an acid-promoted Friedel–Crafts alkylation, **117** and **118** were treated with triflimide in nitromethane to give full conversion to an isomeric product mixture. The electron-withdrawing fluorine substituent led to more effective suppression of reaction at the benzenoid ring than a methyl substituent. Although the Friedel–Crafts macrocyclization approach has the potential to generate libraries of macrocycle isomers that would otherwise be more time consuming to synthesize individually, it was demonstrated that specific isomers can also be prepared convergently (Scheme 13b). Intramolecular Pd^0-catalyzed allylation of 5-fluoro-L-tryptophan methyl ester **122** and cinnamyl alcohol **121** gave *endo*-pyrroloindoline **123**. Two further amino acids were then introduced, followed by deprotection of acid labile protecting groups and lactamization with HBTU. Both products **120d** and **125** were spectroscopically identical.

^{18}F labeling of macrocyclic peptides

Positron emission tomography (PET) is a non-invasive medical diagnostic tool for the detection and diagnosis of diseases by visualizing metabolic processes. Receptor-targeting peptide-based imaging agents possess favorable properties such as high affinities and specificities for their targets, improved pharmacokinetic properties, and biosafety.[117] Furthermore, the biological half-life of many peptides matches the half-life of radionucleotide ^{18}F (109.77 min). Linear Arg-Gly-Asp (RGD) peptides are often prone to enzymatic degradation, while cyclization has been demonstrated to improve *in vivo* stabilities. For instance, Davis *et al.* reported the on-resin head-to-tail cyclization and ^{18}F-radiolabeling of a cyclic peptide, c(RGDyK), a ligand of integrin α$_v$β$_3$ receptors.[118] The acid-sensitive Novasyn® TGA resin was selected to maintain short cleavage times following the on-resin radiolabeling step. Radiolabeling was achieved using a 30 min coupling of [^{18}F]fluorobenzoic acid ([^{18}F]FBA, **126**) to the peptidyl-resin **127** (Scheme 14a). This was followed by a 30 min global deprotection and cleavage to obtain the labeled cyclic peptide **128**.

Chemoselective radio-deoxyfluorination with [^{18}F]fluoride enabled the radiolabeling of peptides containing tyrosine resi-

Scheme 11 Synthesis of fluorine-containing α,γ-cyclic peptides **112** and **114**.

This journal is © the Partner Organisations 2025

Org. Chem. Front., 2025, **12**, 4871–4895 | **4885**
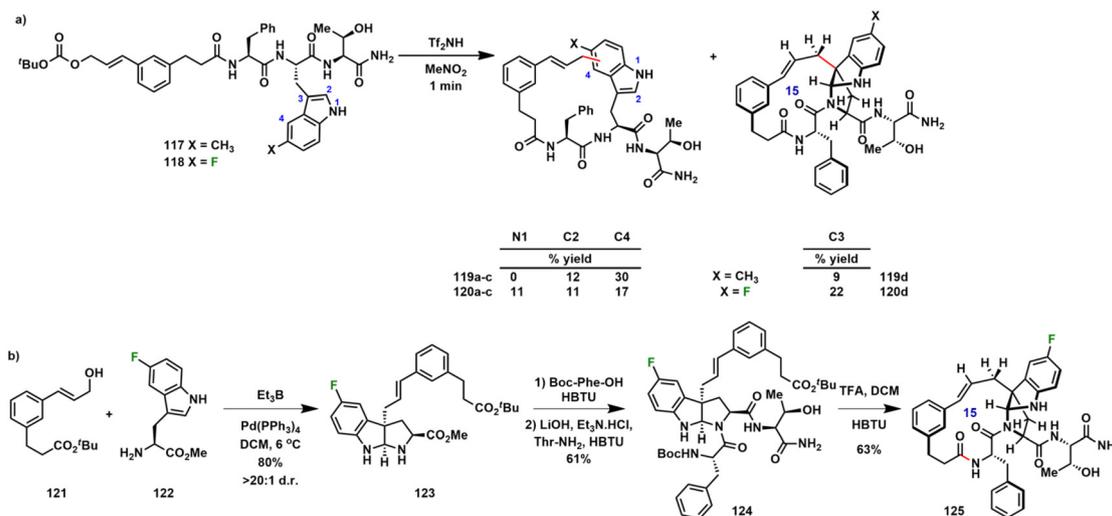
Scheme 13 Pyrroloindoline-forming macrocyclization of 5-fluoro-L-tryptophan by (a) acidolysis to promote internal substitution at N1, C2, C3 or C4 and (b) convergent synthesis.

Scheme 14 (a) On-resin ^{18}F-radiolabeling of macrocyclic RGD pentapeptide **127**. (b) Direct ^{18}F-radiolabeling of macrocyclic RGD-pentapeptide **130**. (c) ^{18}F-radiolabeling of macrocyclic peptides **133a,b** using an ^{18}F version of Umemoto's reagent (**132**).

dues bearing a traceless ruthenium activating group (Scheme 14b).[119] Metal-mediated ^{18}F-radiofluorination has been reviewed elsewhere.[120] A cyclic peptide containing the RGD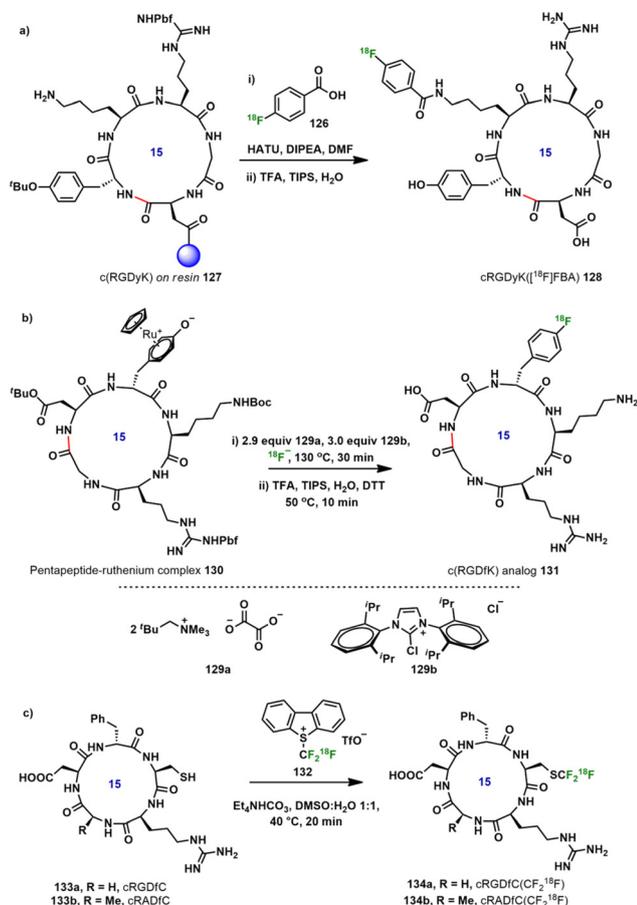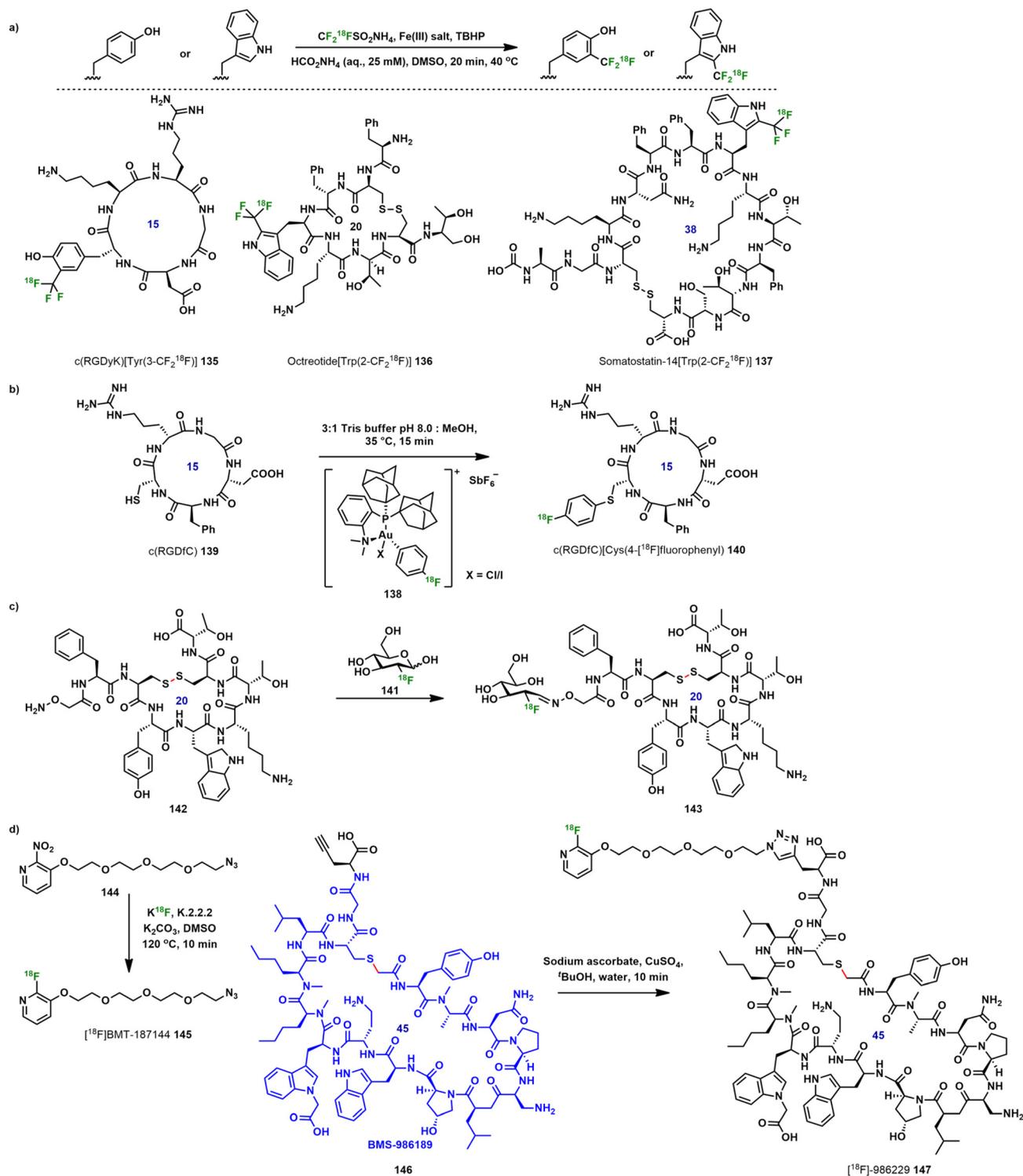 motif was labeled in 25% decay-corrected radiochemical yield (RCY) after purification by HPLC. The source of [^{18}F]fluoride in typical radiolabeling procedures is an aqueous solution of [^{18}F]fluoride trapped on an anion exchange cartridge, with azeotropic drying of the fluoride. This report developed a strategy involving direct elution with the peptide-ruthenium complex in an ethanol-pivalonitrile solvent system, thereby avoiding the need for aqueous elution and azeodrying. The use of bis(trimethylneopentylammonium) oxalate **129a** was vital for successful elution as it increased radiolabeling efficiency 1.7-fold.

[18]F-trifluoromethylation of peptides bearing cysteine residues was achieved using an ^{18}F-labeled version of Umemoto's reagent (**132**) and commercial RGD or RAD pentapeptides (Scheme 14c).[121] Radiolabeled cyclic peptides cRGDfC(CF$_2$[18]F) **134a** and cRADfC(CF$_2$[18]F) **134b** were purified and isolated in 19% ± 5% RCY and 33% ± 9% RCY, respectively.

Kee *et al.* reported the ^{18}F-trifluoromethylation of native aromatic peptide residues using ^{18}F-trifluoromethanesulfinate (CF$_2$[18]FSO$_2$NH$_4$).[122] The ^{18}F reagent was prepared in a single step from K[18]F/K$_{222}$, a difluorocarbene reagent, and a source of SO$_2$. After initial ^{18}F-labeling of dipeptides, the substrate scope for C–H ^{18}F-trifluoromethylation of Tyr and Trp residues was expanded to biologically active macrocyclic peptides (Scheme 15a). The integrin $\alpha_v\beta_3$ receptor ligand c(RGDyK) underwent ^{18}F labeling at 33% radiochemical conversion (RCC). Octreotide, an octapeptidic mimic of somatostatin, underwent ^{18}F-trifluoromethylation in 29% RCC. Somatostatin-14, a macrocyclic tetradecapeptide with broad antisecretory activity on endocrine hormones, was Trp-selectively ^{18}F-labeled in 20% RCY.[122,123] An automated radio-

4886 | *Org. Chem. Front.*, 2025, **12**, 4871–4895

This journal is © the Partner Organisations 2025

Scheme 15 (a) Synthesis of ^{18}F-labeled macrocyclic peptides 135–137. (b) ^{18}F-radiolabeling of a cyclic RGD peptide 139 with organometallic gold (III) reagent 138. (c) Radiolabeling of aminooxy-functionalized octreotate derivative 142 with [^{18}F]FDG 141. (d) Synthesis of ^{18}F-labeled BMS-986229 (147) via CuACC.

synthesis of octreotide[Trp(2-CF$_2$^{18}F)] 136 was also reported with 133 min total synthesis time from [^{18}F]fluoride, which enabled an *in vivo* PET imaging experiment on rats.[122]

^{18}F-labeling of unprotected peptides with an organometallic gold(III) reagent 138 in aqueous media was reported by McDaniel *et al.* (Scheme 15b).[124] A commercially available

cyclic RGD peptide **139** was ^{18}F-radiolabeled to demonstrate that *S*-arylation can be achieved when the Cys residue is in an interchain position. The product **140** was obtained in 94% RCY.

There are challenges associated with the radiolabeling of peptides with the short-lived ^{18}F isotope, due to the large amounts of peptide labeling precursors required as well as extended reaction times. To address these issues, a microfluidic methodology was reported for the radiosynthesis of a clinically relevant octreotate derivative.[125] Octreotate is a somatostatin analog, closely related to octreotide which has a terminal Thr reduced to the corresponding amino alcohol. High decay-corrected RCY values of greater than 82% were obtained for the radiolabeling of the aminooxy-functionalized octreotate derivative **142** with [^{18}F]fluorodeoxyglucose ([^{18}F]FDG, **141**) (Scheme 15c), compared with 76% RCY obtained *via* the conventional non-microfluidic method. The reaction time was shortened from 70 to 30 min, which included its HPLC purification. The microfluidic set-up could be tuned to the required radioactivity level for specific patient doses and, in principle, demonstrated the feasibility of this technology toward clinical applications.[126]

BMS reported the discovery and evaluation of BMS-986229 (**147**), a novel ^{18}F-labeled macrocyclic peptide radioligand for PET imaging and measurement of PD-L1 expression in tumors (Scheme 15d).[127] The programmed death protein (PD-1) is a negative co-stimulatory receptor expressed on activated T- and B-cell surfaces, and PD-L1 is a surface glycoprotein ligand for PD-1.[127] Binding of PD-L1 and PD-1 enables immunosuppression on antigen-presenting cells and human cancers by downregulation of T-cell activation and cytokine secretion. The macrocyclic peptide component of **147** was designed using BMS-986189 (highlighted in Scheme 15d), a fully optimized potent PD-L1 antagonist with picomolar affinity.[128] A propargyl glycine group was incorporated, which enabled copper-catalyzed azide–alkyne cycloaddition (CuAAC) between peptide **146** and [^{18}F]BMT-187144 (**145**) to rapidly label the macrocyclic peptide with [18]F. A non-decayed corrected RCY of 11% was obtained. *In vivo* PET imaging in xenograft models showed an increased uptake of BMS-986229 (**147**) compared to the control. Furthermore, **147** showed a long dissociation off-rate from PD-L1, rapid clearance from the blood and non-PD-L1 tissues, and the largest dynamic range within the non-human primate spleen compared to other PET imaging agents (adnectin and mAb platforms), emphasizing the advantages of using a macrocyclic peptide scaffold.

Conclusions

Fluorine-containing macrocyclic peptides have made a significant impact on medicinal chemistry. The largest category of therapeutic fluorinated macrocyclic peptides are the HCV protease inhibitors. These are 14–18-membered macrocyclic rings, and structures with up to four fluorine atoms have been reported. Other diseases targeted by fluorinated macrocyclic

peptides include hypercholesterolemia (MK-0616, **63**) and various types of cancer (motixafortide, **65**, LUNA18, **66**). Fluorine-specific interactions have led to improved enzyme inhibitory activity, increased metabolic stability and decreased susceptibility to degradation.

Fluorine-containing non-natural amino acids, such as fluoro-Trp, -Tyr and -Phe, have served as useful building blocks for incorporation into macrocyclic peptides. Structures including **63**, **72**, **82**, **125** and **135–137** have benefited from this synthetic strategy. More complex targets include fluorinated bicyclic peptides such as **72**, **75e** and **94**. A common strategy for bicyclization has involved the reaction of Cys residues with specific linkers. Fluoroaromatic linkers such as decafluorodiphenylsulfone (DFS) and decafluorobiphenyl (DFB) have enabled the construction of macrocyclic and bicyclic peptides, while the presence of perfluoroaryl has been shown to increase peptide stability and delivery of antisense oligonucleotides to cells, and to improve delivery of Pt(IV) prodrugs across the blood–brain barrier.[97,99]

mRNA display technology has emerged as a tool for generating large libraries of macrocyclic peptides incorporating non-canonical amino acids.[81,88] This technology allows for the rapid selection of high-affinity macrocyclic peptides containing modified backbones, based on target binding. Notable fluorine-containing examples that have been discovered include inhibitors of EphA2, SIRT2 and thrombin.[80,85,87]

Macrocyclic peptide-based PD-L1 antagonists have been evaluated as PET imaging agents.[129] They are advantageous scaffolds for the design of potential PET ligands due to the opportunities for optimization toward high target affinity and rapid tumor uptake. Peptide-based imaging agents also show rapid clearance from blood and background tissues. Additionally, the site-specific modification of peptides enables facile incorporation of radionuclides.

Despite the numerous benefits of fluorine incorporation into drug leads, it is important to consider the potentially unpredictable effects of fluorine within biological systems. Aromatic fluorination is a well-established strategy to slow metabolism, although aryl fluorides may still undergo oxidative defluorination by enzymes such as cytochrome P450, generating phenolic metabolites and fluoride. In BMS-986144 (**56**), the trifluorinated Boc group lowered the propensity toward metabolism which had afflicted the non-fluorinated, acyclic precursor asunaprevir.[50] Nevertheless, the gain in stability needs to be considered against the toxicity of metabolites from defluorination of macrocyclic peptides.[130] Appropriate and precise placement of the fluorine atom will avoid such issues. As noted in previous literature, the challenge within peptide chemistry lies in the ability to balance the specific properties of the fluorine atom with its behavior in its environment and the impact upon uptake and metabolism.[28]

It is expected that, given their increased drug-likeness, improved proteolytic stability and unique effects on protein–protein interactions, macrocyclic peptides will continue to make an impact on peptide therapeutics. The remarkable and diverse effects of fluorine upon biological molecules have

4888 | *Org. Chem. Front.*, 2025, **12**, 4871–4895

This journal is © the Partner Organisations 2025

forged a vital role within the pharmaceutical industry. We anticipate that the combination of these two fields will continue to strengthen the medicinal chemists' toolbox.

Author contributions

N. R. suggested the concept for this review article and designed its figures and schemes. N. R. and S. R. prepared, edited and reviewed the manuscript. All authors have read and approved the final version.

Data availability

No primary research results, software or code have been included, and no new data were generated or analyzed as part of this review.

Conflicts of interest

There are no conflicts to declare.

Acknowledgements

References

1 A. A. Vinogradov, Y. Yin and H. Suga, Macrocyclic Peptides as Drug Candidates: Recent Progress and Remaining Challenges, *J. Am. Chem. Soc.*, 2019, **141**, 4167–4181.

2 A. K. Yudin, Macrocycles: lessons from the distant past, recent developments, and future directions, *Chem. Sci.*, 2015, **6**, 30–49.

3 PepTherDia, **https://peptherdia.herokuapp.com**, (Accessed Dec 2024).

4 V. D'Aloisio, P. Dognini, G. A. Hutcheon and C. R. Coxon, PepTherDia: database and structural composition analysis of approved peptide therapeutics and diagnostics, *Drug Discovery Today*, 2021, **26**, 1409–1419.

5 E. M. Driggers, S. P. Hale, J. Lee and N. K. Terrett, The exploration of macrocycles for drug discovery—an under-exploited structural class, *Nat. Rev. Drug Discovery*, 2008, **7**, 608–624.

6 C. Lamers, Overcoming the shortcomings of peptide-based therapeutics, *Future Drug Discovery*, 2022, **4**, FDD75.

7 C. Adessi and C. Soto, Converting a Peptide into a Drug: Strategies to Improve Stability and Bioavailability, *Curr. Med. Chem.*, 2002, **9**, 963–978.

8 C. J. White and A. K. Yudin, Contemporary strategies for peptide macrocyclization, *Nat. Chem.*, 2011, **3**, 509–524.

9 Y. H. Lau, P. de Andrade, Y. Wu and D. R. Spring, Peptide stapling techniques based on different macrocyclisation chemistries, *Chem. Soc. Rev.*, 2015, **44**, 91–102.

10 J. Wu, J. Tang, H. Chen, Y. He, H. Wang and H. Yao, Recent developments in peptide macrocyclization, *Tetrahedron Lett.*, 2018, **59**, 325–333.

11 L. A. Viarengo-Baker, L. E. Brown, A. A. Rzepiela and A. Whitty, Defining and navigating macrocycle chemical space, *Chem. Sci.*, 2021, **12**, 4309–4328.

12 S. E. Gibson and C. Lecci, Amino Acid Derived Macrocycles—An Area Driven by Synthesis or Application?, *Angew. Chem., Int. Ed.*, 2006, **45**, 1364–1377.

13 M. Inoue, Y. Sumii and N. Shibata, Contribution of Organofluorine Compounds to Pharmaceuticals, *ACS Omega*, 2020, **5**, 10633–10640.

14 P. Shah and A. D. Westwell, The role of fluorine in medicinal chemistry: Review Article, *J. Enzyme Inhib. Med. Chem.*, 2007, **22**, 527–540.

15 E. P. Gillis, K. J. Eastman, M. D. Hill, D. J. Donnelly and N. A. Meanwell, Applications of Fluorine in Medicinal Chemistry, *J. Med. Chem.*, 2015, **58**, 8315–8359.

16 E. A. Villar, D. Beglov, S. Chennamadhavuni, J. A. Porco, D. Kozakov, S. Vajda and A. Whitty, How proteins bind macrocycles, *Nat. Chem. Biol.*, 2014, **10**, 723–731.

17 R. J. Glyn and G. Pattison, Effects of Replacing Oxygenated Functionality with Fluorine on Lipophilicity, *J. Med. Chem.*, 2021, **64**, 10246–10259.

18 K. Müller, C. Faeh and F. Diederich, Fluorine in Pharmaceuticals: Looking Beyond Intuition, *Science*, 2007, **317**, 1881–1886.

19 N. Rozatian and D. R. W. Hodgson, Reactivities of electrophilic N–F fluorinating reagents, *Chem. Commun.*, 2021, **57**, 683–712.

20 J. Wu, Review of recent advances in nucleophilic C–F bond-forming reactions at sp3 centers, *Tetrahedron Lett.*, 2014, **55**, 4289–4294.

21 Z. Zou, W. Zhang, Y. Wang and Y. Pan, Recent advances in electrochemically driven radical fluorination and fluoroalkylation, *Org. Chem. Front.*, 2021, **8**, 2786–2798.

22 B. Lantaño and A. Postigo, Radical fluorination reactions by thermal and photoinduced methods, *Org. Biomol. Chem.*, 2017, **15**, 9954–9973.

23 S. Barata-Vallejo, B. Lantaño and A. Postigo, Recent Advances in Trifluoromethylation Reactions with Electrophilic Trifluoromethylating Reagents, *Chem. – Eur. J.*, 2014, **20**, 16806–16829.

24 J. Charpentier, N. Früh and A. Togni, Electrophilic Trifluoromethylation by Use of Hypervalent Iodine Reagents, *Chem. Rev.*, 2015, **115**, 650–682.

25 A. Harsanyi and G. Sandford, Organofluorine chemistry: applications, sources and sustainability, *Green Chem.*, 2015, **17**, 2081–2086.

26 C. M. Marshall, J. G. Federice, C. N. Bell, P. B. Cox and J. T. Njardarson, An Update on the Nitrogen Heterocycle

This journal is © the Partner Organisations 2025

Org. Chem. Front., 2025, **12**, 4871–4895 | **4889**

Compositions and Properties of U.S. FDA-Approved Pharmaceuticals (2013–2023), *J. Med. Chem.*, 2024, **67**, 11622–11655.

27 M. Salwiczek, E. K. Nyakatura, U. I. M. Gerling, S. Ye and B. Koksch, Fluorinated amino acids: compatibility with native protein structures and effects on protein–protein interactions, *Chem. Soc. Rev.*, 2012, **41**, 2135–2171.

28 A. A. Berger, J.-S. Völler, N. Budisa and B. Koksch, Deciphering the Fluorine Code—The Many Hats Fluorine Wears in a Protein Environment, *Acc. Chem. Res.*, 2017, **50**, 2093–2103.

29 S. Huhmann and B. Koksch, Fine-Tuning the Proteolytic Stability of Peptides with Fluorinated Amino Acids: Fine-Tuning the Proteolytic Stability of Peptides with Fluorinated Amino Acids, *Eur. J. Org. Chem.*, 2018, 3667–3679.

30 W. D. G. Brittain, C. M. Lloyd and S. L. Cobb, Synthesis of complex unnatural fluorine-containing amino acids, *J. Fluor. Chem.*, 2020, **239**, 109630.

31 J. G. Taylor, S. Zipfel, K. Ramey, R. Vivian, A. Schrier, K. K. Karki, A. Katana, D. Kato, T. Kobayashi, R. Martinez, M. Sangi, D. Siegel, C. V. Tran, Z.-Y. Yang, J. Zablocki, C. Y. Yang, Y. Wang, K. Wang, K. Chan, O. Barauskas, G. Cheng, D. Jin, B. E. Schultz, T. Appleby, A. G. Villaseñor and J. O. Link, Discovery of the pan-genotypic hepatitis C virus NS3/4A protease inhibitor voxilaprevir (GS-9857): A component of Vosevi®, *Bioorg. Med. Chem. Lett.*, 2019, **29**, 2428–2436.

32 Y. N. Lamb, Glecaprevir/Pibrentasvir: First Global Approval, *Drugs*, 2017, **77**, 1797–1804.

33 P. Lampertico, J. A. Carrión, M. Curry, J. Turnes, M. Cornberg, F. Negro, A. Brown, M. Persico, N. Wick, A. Porcalla, A. Pangerl, E. Crown, L. Larsen, Y. Yu and H. Wedemeyer, Real-world effectiveness and safety of glecaprevir/pibrentasvir for the treatment of patients with chronic HCV infection: A meta-analysis, *J. Hepatol.*, 2020, **72**, 1112–1121.

34 J. Han, A. M. Remete, L. S. Dobson, L. Kiss, K. Izawa, H. Moriwaki, V. A. Soloshonok and D. O'Hagan, Next generation organofluorine containing blockbuster drugs, *J. Fluor. Chem.*, 2020, **239**, 109639.

35 R. D. Cink, K. A. Lukin, R. D. Bishop, G. Zhao, M. J. Pelc, T. B. Towne, B. D. Gates, M. M. Ravn, D. R. Hill, C. Ding, S. C. Cullen, J. Mei, M. R. Leanna, J. Henle, J. G. Napolitano, N. K. Nere, S. Chen, A. Sheikh and J. M. Kallemeyn, Development of the Enabling Route for Glecaprevir via Ring-Closing Metathesis, *Org. Process Res. Dev.*, 2020, **24**, 183–200.

36 D. R. Hill, M. J. Abrahamson, K. A. Lukin, T. B. Towne, K. M. Engstrom, R. E. Reddy, A. B. Kielbus, M. J. Pelc, J. Mei, N. K. Nere, S. Chen, R. Henry, S. Chemburkar, C. Ding, H. Zhang and R. D. Cink, Development of a Large-Scale Route to Glecaprevir: Synthesis of the Side Chain and Final Assembly, *Org. Process Res. Dev.*, 2020, **24**, 1393–1404.

37 S. Zeuzem, G. R. Foster, S. Wang, A. Asatryan, E. Gane, J. J. Feld, T. Asselah, M. Bourlière, P. J. Ruane, H. Wedemeyer, S. Pol, R. Flisiak, F. Poordad, W.-L. Chuang, C. A. Stedman, S. Flamm, P. Kwo, G. J. Dore, G. Sepulveda-Arzola, S. K. Roberts, R. Soto-Malave, K. Kaita, M. Puoti, J. Vierling, E. Tam, H. E. Vargas, R. Bruck, F. Fuster, S.-W. Paik, F. Felizarta, J. Kort, B. Fu, R. Liu, T. I. Ng, T. Pilot-Matias, C.-W. Lin, R. Trinh and F. J. Mensa, Glecaprevir–Pibrentasvir for 8 or 12 Weeks in HCV Genotype 1 or 3 Infection, *N. Engl. J. Med.*, 2018, **378**, 354–369.

38 J. Zephyr, N. Kurt Yilmaz and C. A. Schiffer, Viral proteases: Structure, mechanism and inhibition, in *The Enzymes*, Elsevier, 2021, vol. 50, pp. 301–333.

39 J. Timm, K. Kosovrasti, M. Henes, F. Leidner, S. Hou, A. Ali, N. Kurt Yilmaz and C. A. Schiffer, Molecular and Structural Mechanism of Pan-Genotypic HCV NS3/4A Protease Inhibition by Glecaprevir, *ACS Chem. Biol.*, 2020, **15**, 342–352.

40 J. Zephyr, D. Nageswara Rao, S. V. Vo, M. Henes, K. Kosovrasti, A. N. Matthew, A. K. Hedger, J. Timm, E. T. Chan, A. Ali, N. Kurt Yilmaz and C. A. Schiffer, Deciphering the Molecular Mechanism of HCV Protease Inhibitor Fluorination as a General Approach to Avoid Drug Resistance, *J. Mol. Biol.*, 2022, **434**, 167503.

41 D. Nageswara Rao, J. Zephyr, M. Henes, E. T. Chan, A. N. Matthew, A. K. Hedger, H. L. Conway, M. Saeed, A. Newton, C. J. Petropoulos, W. Huang, N. Kurt Yilmaz, C. A. Schiffer and A. Ali, Discovery of Quinoxaline-Based P1–P3 Macrocyclic NS3/4A Protease Inhibitors with Potent Activity against Drug-Resistant Hepatitis C Virus Variants, *J. Med. Chem.*, 2021, **64**, 11972–11989.

42 Y. Jiang, S. W. Andrews, K. R. Condroski, B. Buckman, V. Serebryany, S. Wenglowsky, A. L. Kennedy, M. R. Madduru, B. Wang, M. Lyon, G. A. Doherty, B. T. Woodard, C. Lemieux, M. G. Do, H. Zhang, J. Ballard, G. Vigers, B. J. Brandhuber, P. Stengel, J. A. Josey, L. Beigelman, L. Blatt and S. D. Seiwert, Discovery of Danoprevir (ITMN-191/R7227), a Highly Selective and Potent Inhibitor of Hepatitis C Virus (HCV) NS3/4A Protease, *J. Med. Chem.*, 2014, **57**, 1753–1769.

43 S. D. Seiwert, S. W. Andrews, Y. Jiang, V. Serebryany, H. Tan, K. Kossen, P. T. R. Rajagopalan, S. Misialek, S. K. Stevens, A. Stoycheva, J. Hong, S. R. Lim, X. Qin, R. Rieger, K. R. Condroski, H. Zhang, M. G. Do, C. Lemieux, G. P. Hingorani, D. P. Hartley, J. A. Josey, L. Pan, L. Beigelman and L. M. Blatt, Preclinical Characteristics of the Hepatitis C Virus NS3/4A Protease Inhibitor ITMN-191 (R7227), *Antimicrob. Agents Chemother.*, 2008, **52**, 4432–4441.

44 H. Chen, Z. Zhang, L. Wang, Z. Huang, F. Gong, X. Li, Y. Chen and J. J. Wu, First clinical study using HCV protease inhibitor danoprevir to treat COVID-19 patients, *Medicine*, 2020, **99**, e23357.

45 Z. Zhang, S. Wang, X. Tu, X. Peng, Y. Huang, L. Wang, W. Ju, J. Rao, X. Li, D. Zhu, H. Sun and H. Chen, A comparative study on the time to achieve negative nucleic acid testing and hospital stays between danoprevir and lopina-

4890 | *Org. Chem. Front.*, 2025, **12**, 4871–4895

This journal is © the Partner Organisations 2025

vir/ritonavir in the treatment of patients with COVID–19, *J. Med. Virol.*, 2020, **92**, 2631–2636.

46 A. Vaidya and C. M. Perry, Simeprevir: First Global Approval, *Drugs*, 2013, **73**, 2093–2106.

47 G. Milanole, F. Andriessen, G. Lemonnier, M. Sebban, G. Coadou, S. Couve-Bonnaire, J.-F. Bonfanti, P. Jubault and X. Pannecoucke, Toward the Synthesis of Fluorinated Analogues of HCV NS3/4A Serine Protease Inhibitors Using Methyl α-Amino-β-fluoro-β-vinylcyclopropanecarboxylate as Key Intermediate, *Org. Lett.*, 2015, **17**, 2968–2971.

48 K. F. McDaniel, H. Chen, M. Yeung, T. Middleton, L. Lu and K. Kurtz, Macrocyclic Hepatitis C Serine Protease Inhibitors, *WO Pat.*, WO2012092409A2, 2012.

49 M. Smith and A. Lim, Profile of paritaprevir/ritonavir/ombitasvir plus dasabuvir in the treatment of chronic hepatitis C virus genotype 1 infection, *Drug Des., Dev. Ther.*, 2015, 6083.

50 L.-Q. Sun, E. Mull, S. D'Andrea, B. Zheng, S. Hiebert, E. Gillis, M. Bowsher, S. Kandhasamy, V. R. Baratam, S. Puttaswamy, N. Pulicharla, S. Vishwakrishnan, S. Reddy, R. Trivedi, S. Sinha, S. Sivaprasad, A. Rao, S. Desai, K. Ghosh, R. Anumula, A. Kumar, R. Rajamani, Y.-K. Wang, H. Fang, A. Mathur, R. Rampulla, T. A. Zvyaga, K. Mosure, S. Jenkins, P. Falk, D. M. Tagore, C. Chen, K. Rendunchintala, J. Loy, N. A. Meanwell, F. McPhee and P. M. Scola, Discovery of BMS-986144, a Third-Generation, Pan-Genotype NS3/4A Protease Inhibitor for the Treatment of Hepatitis C Virus Infection, *J. Med. Chem.*, 2020, **63**, 14740–14760.

51 L.-Q. Sun, E. Mull, B. Zheng, S. D'Andrea, Q. Zhao, A. X. Wang, N. Sin, B. L. Venables, S.-Y. Sit, Y. Chen, J. Chen, A. Cocuzza, D. M. Bilder, A. Mathur, R. Rampulla, B.-C. Chen, T. Palani, S. Ganesan, P. N. Arunachalam, P. Falk, S. Levine, C. Chen, J. Friborg, F. Yu, D. Hernandez, A. K. Sheaffer, J. O. Knipe, Y.-H. Han, R. Schartman, M. Donoso, K. Mosure, M. W. Sinz, T. Zvyaga, R. Rajamani, K. Kish, J. Tredup, H. E. Klei, Q. Gao, A. Ng, L. Mueller, D. M. Grasela, S. Adams, J. Loy, P. C. Levesque, H. Sun, H. Shi, L. Sun, W. Warner, D. Li, J. Zhu, Y.-K. Wang, H. Fang, M. I. Cockett, N. A. Meanwell, F. McPhee and P. M. Scola, Discovery of a Potent Acyclic, Tripeptidic, Acyl Sulfonamide Inhibitor of Hepatitis C Virus NS3 Protease as a Back-up to Asunaprevir with the Potential for Once-Daily Dosing, *J. Med. Chem.*, 2016, **59**, 8042–8060.

52 S. F. Neelamkavil, S. Agrawal, T. Bara, C. Bennett, S. Bhat, D. Biswas, L. Brockunier, N. Buist, D. Burnette, M. Cartwright, S. Chackalamannil, R. Chase, M. Chelliah, A. Chen, M. Clasby, V. J. Colandrea, I. W. Davies, K. Eagen, Z. Guo, Y. Han, J. Howe, C. Jayne, H. Josien, S. Kargman, K. Marcantonio, S. Miao, R. Miller, A. Nolting, P. Pinto, M. Rajagopalan, R. T. Ruck, U. Shah, A. Soriano, D. Sperbeck, F. Velazquez, J. Wu, Y. Xia and S. Venkatraman, Discovery of MK-8831, A Novel Spiro-Proline Macrocycle as a Pan-Genotypic HCV-NS3/4a

Protease Inhibitor, *ACS Med. Chem. Lett.*, 2016, **7**, 111–116.

53 X. C. Sheng, A. Casarez, R. Cai, M. O. Clarke, X. Chen, A. Cho, W. E. Delaney, E. Doerffler, M. Ji, M. Mertzman, R. Pakdaman, H.-J. Pyun, T. Rowe, Q. Wu, J. Xu and C. U. Kim, Discovery of GS-9256: A novel phosphinic acid derived inhibitor of the hepatitis C virus NS3/4A protease with potent clinical activity, *Bioorg. Med. Chem. Lett.*, 2012, **22**, 1394–1396.

54 H. Yang, C. Yang, Y. Wang, G. Rhodes, M. Robinson, G. Cheng, X. Qi, H. Mo, Y. Tian, R. Pakdaman, X. C. Sheng, C. U. Kim and W. E. Delaney, Preclinical Characterization of the Novel HCV NS3 Protease Inhibitor GS-9256, *Antiviral Ther.*, 2017, **22**, 413–420.

55 E. De Clercq, Current race in the development of DAAs (direct-acting antivirals) against HCV, *Biochem. Pharmacol.*, 2014, **89**, 441–452.

56 J. A. McCauley and M. T. Rudd, Hepatitis C virus NS3/4a protease inhibitors, *Curr. Opin. Pharmacol.*, 2016, **30**, 84–92.

57 J. Arumugasamy, K. Arunachalam, D. Bauer, A. Becker, C. A. Caillet, R. Glynn, G. M. Latham, J. Lim, J. Liu, B. A. Mayes, A. Moussa, E. Rosinovsky, A. E. Salanson, A. F. Soret, A. Stewart, J. Wang and X. Wu, Development of Related HCV Protease Inhibitors: Macrocyclization of Two Highly Functionalized Dienyl-ureas via Ring-Closing Metathesis, *Org. Process Res. Dev.*, 2013, **17**, 811–828.

58 C. C. Parsy, F.-R. Alexandre, V. Bidau, F. Bonnaterre, G. Brandt, C. Caillet, S. Cappelle, D. Chaves, T. Convard, M. Derock, D. Gloux, Y. Griffon, L. B. Lallos, F. Leroy, M. Liuzzi, A.-G. Loi, L. Moulat, M. Chiara, H. Rahali, V. Roques, E. Rosinovsky, S. Savin, M. Seifer, D. Standring and D. Surleraux, Discovery and structural diversity of the hepatitis C virus NS3/4A serine protease inhibitor series leading to clinical candidate IDX320, *Bioorg. Med. Chem. Lett.*, 2015, **25**, 5427–5436.

59 J. De Bruijne, A. Van Vliet, C. J. Weegink, W. Mazur, A. Wiercinska-Drapało, K. Simon, G. Cholewińska-Szymańska, J. Kapocsi, I. Várkonyi, X.-J. Zhou, M.-F. Temam, J. Molles, J. Chen, K. Pietropaolo, J. F. McCarville, J. Z. Sullivan-Bólyai, D. Mayers and H. Reesink, Rapid Decline of Viral RNA in Chronic Hepatitis C Patients Treated Once Daily with IDX320: A Novel Macrocyclic HCV Protease Inhibitor, *Antiviral Ther.*, 2012, **17**, 633–642.

60 D. G. Johns, L.-C. Campeau, P. Banka, A. Bautmans, T. Bueters, E. Bianchi, D. Branca, P. G. Bulger, I. Crevecoeur, F.-X. Ding, R. M. Garbaccio, E. D. Guetschow, Y. Guo, S. N. Ha, J. M. Johnston, H. Josien, E. A. Kauh, K. A. Koeplinger, J. T. Kuethe, E. Lai, C. L. Lanning, A. Y. H. Lee, L. Li, A. G. Nair, E. A. O'Neill, S. A. Stoch, D. A. Thaisrivongs, T. J. Tucker, P. Vachal, K. Van Dyck, F. P. Vanhoutte, B. Volckaert, D. G. Wolford, A. Xu, T. Zhao, D. Zhou, S. Zhou, X. Zhu, H. J. Zokian, A. M. Walji and H. B. Wood, Orally Bioavailable Macrocyclic Peptide That Inhibits Binding of

This journal is © the Partner Organisations 2025

Org. Chem. Front., 2025, **12**, 4871–4895 | **4891**

PCSK9 to the Low Density Lipoprotein Receptor, *Circulation*, 2023, **148**, 144–158.

61 D. G. Johns, P. Banka, Z. Zhou, A. Klapara, F. Tsay, J. Kong, R. J. Varsolona, R. Desmond, P. E. Maligres, M. Marota, C. Alleyne, G. A. Okoh, J. C. Dinunzio, R. Nofsinger, L. Li, D. J. Smith, M. Mahjour, K. A. Koeplinger, Y. Xiong, P. W. Wuefling and D. J. Higgins, Compounds for treating conditions related to PCSK9 activity, *WO Pat.*, WO2023023245A1, 2023.

62 https://drughunter.com/articles/mk-0616-the-2023-mole-cule-of-the-year (Accessed Sep 2024).

63 C. M. Ballantyne, P. Banka, G. Mendez, R. Garcia, J. Rosenstock, A. Rodgers, G. Mendizabal, Y. Mitchel and A. L. Catapano, Phase 2b Randomized Trial of the Oral PCSK9 Inhibitor MK-0616, *J. Am. Coll. Cardiol.*, 2023, **81**, 1553–1564.

64 T. J. Tucker, M. W. Embrey, C. Alleyne, R. P. Amin, A. Bass, B. Bhatt, E. Bianchi, D. Branca, T. Bueters, N. Buist, S. N. Ha, M. Hafey, H. He, J. Higgins, D. G. Johns, A. D. Kerekes, K. A. Koeplinger, J. T. Kuethe, N. Li, B. Murphy, P. Orth, S. Salowe, A. Shahripour, R. Tracy, W. Wang, C. Wu, Y. Xiong, H. J. Zokian, H. B. Wood and A. Walji, A Series of Novel, Highly Potent, and Orally Bioavailable Next-Generation Tricyclic Peptide PCSK9 Inhibitors, *J. Med. Chem.*, 2021, **64**, 16770–16800.

65 S. M. Hoy, Motixafortide: First Approval, *Drugs*, 2023, **83**, 1635–1643.

66 M. Tanada, M. Tamiya, A. Matsuo, A. Chiyoda, K. Takano, T. Ito, M. Irie, T. Kotake, R. Takeyama, H. Kawada, R. Hayashi, S. Ishikawa, K. Nomura, N. Furuichi, Y. Morita, M. Kage, S. Hashimoto, K. Nii, H. Sase, K. Ohara, A. Ohta, S. Kuramoto, Y. Nishimura, H. Iikura and T. Shiraishi, Development of Orally Bioavailable Peptides Targeting an Intracellular Protein: From a Hit to a Clinical KRAS Inhibitor, *J. Am. Chem. Soc.*, 2023, **145**, 16610–16620.

67 A. Ohta, M. Tanada, S. Shinohara, Y. Morita, K. Nakano, Y. Yamagishi, R. Takano, S. Kariyuki, T. Iida, A. Matsuo, K. Ozeki, T. Emura, Y. Sakurai, K. Takano, A. Higashida, M. Kojima, T. Muraoka, R. Takeyama, T. Kato, K. Kimura, K. Ogawa, K. Ohara, S. Tanaka, Y. Kikuchi, N. Hisada, R. Hayashi, Y. Nishimura, K. Nomura, T. Tachibana, M. Irie, H. Kawada, T. Torizawa, N. Murao, T. Kotake, M. Tanaka, S. Ishikawa, T. Miyake, M. Tamiya, M. Arai, A. Chiyoda, S. Akai, H. Sase, S. Kuramoto, T. Ito, T. Shiraishi, T. Kojima and H. Iikura, Validation of a New Methodology to Create Oral Drugs beyond the Rule of 5 for Intracellular Tough Targets, *J. Am. Chem. Soc.*, 2023, **145**, 24035–24051.

68 H. R. Hoveyda, E. Marsault, R. Gagnon, A. P. Mathieu, M. Vézina, A. Landry, Z. Wang, K. Benakli, S. Beaubien, C. Saint-Louis, M. Brassard, J.-F. Pinault, L. Ouellet, S. Bhat, M. Ramaseshan, X. Peng, L. Foucher, S. Beauchemin, P. Bhérer, D. F. Veber, M. L. Peterson and G. L. Fraser, Optimization of the Potency and Pharmacokinetic Properties of a Macrocyclic Ghrelin Receptor Agonist (Part I): Development of Ulimorelin

(TZP-101) from Hit to Clinic, *J. Med. Chem.*, 2011, **54**, 8305–8320.

69 B. L. Podlogar, R. A. Farr, D. Friedrich, C. Tarnus, E. W. Huber, R. J. Cregge and D. Schirlin, Design, Synthesis, and Conformational Analysis of a Novel Macrocyclic HIV-Protease Inhibitor, *J. Med. Chem.*, 1994, **37**, 3684–3692.

70 M. Boehm, K. Beaumont, R. Jones, A. S. Kalgutkar, L. Zhang, K. Atkinson, G. Bai, J. A. Brown, H. Eng, G. H. Goetz, B. R. Holder, B. Khunte, S. Lazzaro, C. Limberakis, S. Ryu, M. J. Shapiro, L. Tylaska, J. Yan, R. Turner, S. S. F. Leung, M. Ramaseshan, D. A. Price, S. Liras, M. P. Jacobson, D. J. Earp, R. S. Lokey, A. M. Mathiowetz and E. Menhaji-Klotz, Discovery of Potent and Orally Bioavailable Macrocyclic Peptide–Peptoid Hybrid CXCR7 Modulators, *J. Med. Chem.*, 2017, **60**, 9653–9663.

71 F. O. Gombert, A. Lederer, D. Obrecht, B. Romagnoli, C. Bisang and C. Ludin, Template-Fixed Peptidomimetics with CXCR7 Modulating Activity, *WO Pat.*, WO2011095220, 2011.

72 S. J. Middendorp, J. Wilbs, C. Quarroz, S. Calzavarini, A. Angelillo-Scherrer and C. Heinis, Peptide Macrocycle Inhibitor of Coagulation Factor XII with Subnanomolar Affinity and High Target Selectivity, *J. Med. Chem.*, 2017, **60**, 1151–1158.

73 G. A. Pankuch, L. M. Kelly, G. Lin, A. Bryskier, C. Couturier, M. R. Jacobs and P. C. Appelbaum, Activities of a New Oral Streptogramin, XRP 2868, Compared to Those of Other Agents against *Streptococcus pneumoniae* and *Haemophilus* Species, *Antimicrob. Agents Chemother.*, 2003, **47**, 3270–3274.

74 J. Noeske, J. Huang, N. B. Olivier, R. A. Giacobbe, M. Zambrowski and J. H. D. Cate, Synergy of Streptogramin Antibiotics Occurs Independently of Their Effects on Translation, *Antimicrob. Agents Chemother.*, 2014, **58**, 5269–5279.

75 L. Cai, I. B. Seiple and Q. Li, Modular Chemical Synthesis of Streptogramin and Lankacidin Antibiotics, *Acc. Chem. Res.*, 2021, **54**, 1891–1908.

76 D. Sighel, G. Battistini, E. F. Rosatti, J. Vigna, M. Pavan, R. Belli, D. Peroni, F. Alessandrini, S. Longhi, M. Pancher, J. Rorbach, S. Moro, A. Quattrone and I. Mancini, Streptogramin A derivatives as mitochondrial translation inhibitors to suppress glioblastoma stem cell growth, *Eur. J. Med. Chem.*, 2023, **246**, 114979.

77 H. Zhou, L. Liu, J. Huang, D. Bernard, H. Karatas, A. Navarro, M. Lei and S. Wang, Structure-Based Design of High-Affinity Macrocyclic Peptidomimetics to Block the Menin-Mixed Lineage Leukemia 1 (MLL1) Protein–Protein Interaction, *J. Med. Chem.*, 2013, **56**, 1113–1123.

78 T. Tsunemi, S. J. Bernardino, A. Mendoza, C. G. Jones and P. G. Harran, Syntheses of Atypically Fluorinated Peptidyl Macrocycles through Sequential Vinylic Substitutions, *Angew. Chem., Int. Ed.*, 2020, **59**, 674–678.

4892 | *Org. Chem. Front.*, 2025, **12**, 4871–4895

This journal is © the Partner Organisations 2025

79 A. Mendoza, S. J. Bernardino, M. J. Dweck, I. Valencia, D. Evans, H. Tian, W. Lee, Y. Li, K. N. Houk and P. G. Harran, Cascade Synthesis of Fluorinated Spiroheterocyclic Scaffolding for Peptidic Macrobicycles, *J. Am. Chem. Soc.*, 2023, **145**, 15888–15895.

80 J. Morimoto, Y. Hayashi and H. Suga, Discovery of Macrocyclic Peptides Armed with a Mechanism-Based Warhead: Isoform-Selective Inhibition of Human Deacetylase SIRT2, *Angew. Chem., Int. Ed.*, 2012, **51**, 3423–3427.

81 K. Ito, T. Passioura and H. Suga, Technologies for the Synthesis of mRNA-Encoding Libraries and Discovery of Bioactive Natural Product-Inspired Non-Traditional Macrocyclic Peptides, *Molecules*, 2013, **18**, 3502–3528.

82 J. Piekielna, R. Perlikowska, J. C. do-Rego, J.-L. do-Rego, M. C. Cerlesi, G. Calo, A. Kluczyk, K. Łapiński, C. Tömböly and A. Janecka, Synthesis of Mixed Opioid Affinity Cyclic Endomorphin-2 Analogues with Fluorinated Phenylalanines, *ACS Med. Chem. Lett.*, 2015, **6**, 579–583.

83 A. Łęgowska, D. Dębowski, A. Lesner, M. Wysocka and K. Rolka, Introduction of non-natural amino acid residues into the substrate-specific P1 position of trypsin inhibitor SFTI-1 yields potent chymotrypsin and cathepsin G inhibitors, *Bioorg. Med. Chem.*, 2009, **17**, 3302–3307.

84 K. Josephson, M. C. T. Hartman and J. W. Szostak, Ribosomal Synthesis of Unnatural Peptides, *J. Am. Chem. Soc.*, 2005, **127**, 11727–11735.

85 J. Wu, Y. Wang, W. Cai, D. Chen, X. Peng, H. Dong, J. Li, H. Liu, S. Shi, S. Tang, Z. Li, H. Sui, Y. Wang, C. Wu, Y. Zhang, X. Fu and Y. Yin, Ribosomal translation of fluorinated non-canonical amino acids for *de novo* biologically active fluorinated macrocyclic peptides, *Chem. Sci.*, 2024, **15**, 13889–13898.

86 I. R. Mathiesen, E. D. D. Calder, S. Kunzelmann and L. J. Walport, Discovering covalent cyclic peptide inhibitors of peptidyl arginine deiminase 4 (PADI4) using mRNA-display with a genetically encoded electrophilic warhead, *Commun. Chem.*, 2024, **7**, 304.

87 Y. V. Guillen Schlippe, M. C. T. Hartman, K. Josephson and J. W. Szostak, *In Vitro* Selection of Highly Modified Cyclic Peptides That Act as Tight Binding Inhibitors, *J. Am. Chem. Soc.*, 2012, **134**, 10469–10477.

88 K. Josephson, A. Ricardo and J. W. Szostak, mRNA display: from basic principles to macrocycle drug discovery, *Drug Discovery Today*, 2014, **19**, 388–399.

89 M. L. Merz, S. Habeshian, B. Li, J.-A. G. L. David, A. L. Nielsen, X. Ji, K. Il Khwildy, M. M. Duany Benitez, P. Phothirath and C. Heinis, De novo development of small cyclic peptides that are orally bioavailable, *Nat. Chem. Biol.*, 2024, **20**, 624–633.

90 A. M. Spokoyny, Y. Zou, J. J. Ling, H. Yu, Y.-S. Lin and B. L. Pentelute, A Perfluoroaryl-Cysteine SNAr Chemistry Approach to Unprotected Peptide Stapling, *J. Am. Chem. Soc.*, 2013, **135**, 5946–5949.

91 S. J. M. Verhoork, C. E. Jennings, N. Rozatian, J. Reeks, J. Meng, E. K. Corlett, F. Bunglawala, M. E. M. Noble,

A. G. Leach and C. R. Coxon, Tuning the Binding Affinity and Selectivity of Perfluoroaryl–Stapled Peptides by Cysteine–Editing, *Chem. – Eur. J.*, 2019, **25**, 177–182.

92 W. D. G. Brittain and C. R. Coxon, Perfluoroaryl and Perfluoroheteroaryl Reagents as Emerging New Tools for Peptide Synthesis, Modification and Bioconjugation, *Chem. – Eur. J.*, 2022, **28**, e202103305.

93 S. Kalhor-Monfared, M. R. Jafari, J. T. Patterson, P. I. Kitov, J. J. Dwyer, J. M. Nuss and R. Derda, Rapid biocompatible macrocyclization of peptides with decafluorodiphenylsulfone, *Chem. Sci.*, 2016, **7**, 3785–3790.

94 G. Lautrette, F. Touti, H. G. Lee, P. Dai and B. L. Pentelute, Nitrogen Arylation for Macrocyclization of Unprotected Peptides, *J. Am. Chem. Soc.*, 2016, **138**, 8340–8343.

95 A. G. Jamieson, N. Boutard, D. Sabatino and W. D. Lubell, Peptide Scanning for Studying Structure–Activity Relationships in Drug Discovery, *Chem. Biol. Drug Des.*, 2013, **81**, 148–165.

96 Y. Zou, A. M. Spokoyny, C. Zhang, M. D. Simon, H. Yu, Y.-S. Lin and B. L. Pentelute, Convergent diversity-oriented side-chain macrocyclization scan for unprotected polypeptides, *Org. Biomol. Chem.*, 2014, **12**, 566–573.

97 J. M. Wolfe, C. M. Fadzen, R. L. Holden, M. Yao, G. J. Hanson and B. L. Pentelute, Perfluoroaryl Bicyclic Cell–Penetrating Peptides for Delivery of Antisense Oligonucleotides, *Angew. Chem., Int. Ed.*, 2018, **57**, 4756–4759.

98 K. Siva, G. Covello and M. A. Denti, Exon-Skipping Antisense Oligonucleotides to Correct Missplicing in Neurogenetic Diseases, *Nucleic Acid Ther.*, 2014, **24**, 69–86.

99 C. M. Fadzen, J. M. Wolfe, C.-F. Cho, E. A. Chiocca, S. E. Lawler and B. L. Pentelute, Perfluoroarene–Based Peptide Macrocycles to Enhance Penetration Across the Blood–Brain Barrier, *J. Am. Chem. Soc.*, 2017, **139**, 15628–15631.

100 D. Wang and S. J. Lippard, Cellular processing of platinum anticancer drugs, *Nat. Rev. Drug Discovery*, 2005, **4**, 307–320.

101 C. M. Fadzen, J. M. Wolfe, W. Zhou, C.-F. Cho, N. Von Spreckelsen, K. T. Hutchinson, Y.-C. Lee, E. A. Chiocca, S. E. Lawler, O. H. Yilmaz, S. J. Lippard and B. L. Pentelute, A Platinum(ɪᴠ) Prodrug—Perfluoroaryl Macrocyclic Peptide Conjugate Enhances Platinum Uptake in the Brain, *J. Med. Chem.*, 2020, **63**, 6741–6747.

102 P. Wadhwani, S. Afonin, M. Ieronimo, J. Buerck and A. S. Ulrich, Optimized Protocol for Synthesis of Cyclic Gramicidin S: Starting Amino Acid Is Key to High Yield, *J. Org. Chem.*, 2006, **71**, 55–61.

103 J. Salgado, S. L. Grage, L. H. Kondejewski, R. S. Hodges, R. N. McElhaney and A. S. Ulrich, Membrane-bound structure and alignment of the antimicrobial β-sheet peptide gramicidin S derived from angular and distance constraints by solid state 19F-NMR, *J. Biomol. NMR*, 2001, **21**, 191–208.

This journal is © the Partner Organisations 2025

Org. Chem. Front., 2025, **12**, 4871–4895 | **4893**

104 K. Y. Palate, Z. Yang, A. C. Whitwood and W. P. Unsworth, Synthesis of medium-ring lactams and macrocyclic peptide mimetics *via* conjugate addition/ring expansion cascade reactions, *RSC Chem. Biol.*, 2022, **3**, 334–340.

105 J. Y. K. Wong, A. I. Ekanayake, S. Kharchenko, S. E. Kirberger, R. Qiu, P. Kelich, S. Sarkar, J. Li, K. X. Fernandez, E. R. Alvizo-Paez, J. Miao, S. Kalhor-Monfared, J. D. John, H. Kang, H. Choi, J. M. Nuss, J. C. Vederas, Y.-S. Lin, M. S. Macauley, L. Vukovic, W. C. K. Pomerantz and R. Derda, Genetically encoded discovery of perfluoroaryl macrocycles that bind to albumin and exhibit extended circulation in vivo, *Nat. Commun.*, 2023, **14**, 5654.

106 L. Hunter, The C–F bond as a conformational tool in organic and biological chemistry, *Beilstein J. Org. Chem.*, 2010, **6**, 38.

107 X.-G. Hu, D. S. Thomas, R. Griffith and L. Hunter, Stereoselective Fluorination Alters the Geometry of a Cyclic Peptide: Exploration of Backbone-Fluorinated Analogues of Unguisin A, *Angew. Chem., Int. Ed.*, 2014, **53**, 6176–6179.

108 I. Yamamoto, M. J. T. Jordan, N. Gavande, M. R. Doddareddy, M. Chebib and L. Hunter, The enantiomers of syn-2,3-difluoro-4-aminobutyric acid elicit opposite responses at the GABA C receptor, *Chem. Commun.*, 2012, **48**, 829–831.

109 A. D. Ariawan, J. E. A. Webb, E. N. W. Howe, P. A. Gale, P. Thordarson and L. Hunter, Cyclic peptide unguisin A is an anion receptor with high affinity for phosphate and pyrophosphate, *Org. Biomol. Chem.*, 2017, **15**, 2962–2967.

110 N. Díaz and D. Suárez, Understanding the Conformational Properties of Fluorinated Polypeptides: Molecular Modelling of Unguisin A, *J. Chem. Inf. Model.*, 2021, **61**, 223–237.

111 C. Au, C. Gonzalez, Y. C. Leung, F. Mansour, J. Trinh, Z. Wang, X.-G. Hu, R. Griffith, E. Pasquier and L. Hunter, Tuning the properties of a cyclic RGD-containing tetrapeptide through backbone fluorination, *Org. Biomol. Chem.*, 2019, **17**, 664–674.

112 S. S. Burade, T. Saha, N. Bhuma, N. Kumbhar, A. Kotmale, P. R. Rajamohanan, R. G. Gonnade, P. Talukdar and D. D. Dhavale, Self-Assembly of Fluorinated Sugar Amino Acid Derived α,γ-Cyclic Peptides into Transmembrane Anion Transport, *Org. Lett.*, 2017, **19**, 5948–5951.

113 T. J. Cogswell, A. Dahlén and L. Knerr, Synthesis of Diverse α–Fluoroalkoxyaryl Derivatives and Their Use for the Generation of Fluorinated Macrocycles, *Chem. – Eur. J.*, 2018, **25**, 1184–1187.

114 D. O'Hagan, Understanding organofluorine chemistry. An introduction to the C–F bond, *Chem. Soc. Rev.*, 2008, **37**, 308–319.

115 T. E. Rose, B. H. Curtin, K. V. Lawson, A. Simon, K. N. Houk and P. G. Harran, On the prevalence of bridged macrocyclic pyrroloindolines formed in regiodivergent alkylations of tryptophan, *Chem. Sci.*, 2016, **7**, 4158–4166.

116 K. V. Lawson, T. E. Rose and P. G. Harran, Template-induced macrocycle diversity through large ring-forming alkylations of tryptophan, *Tetrahedron*, 2013, **69**, 7683–7691.

117 X. Sun, Y. Li, T. Liu, Z. Li, X. Zhang and X. Chen, Peptide-based imaging agents for cancer detection, *Adv. Drug Delivery Rev.*, 2017, **110–111**, 38–51.

118 R. A. Davis, K. Lau, S. H. Hausner and J. L. Sutcliffe, Solid-phase synthesis and fluorine-18 radiolabeling of cycloRGDyK, *Org. Biomol. Chem.*, 2016, **14**, 8659–8663.

119 J. Rickmeier and T. Ritter, Site–Specific Deoxyfluorination of Small Peptides with [^{18}F]Fluoride, *Angew. Chem., Int. Ed.*, 2018, **57**, 14207–14211.

120 T. G. Luu and H.-K. Kim, Recent progress on radiofluorination using metals: strategies for generation of C–^{18}F bonds, *Org. Chem. Front.*, 2023, **10**, 5746–5781.

121 S. Verhoog, C. W. Kee, Y. Wang, T. Khotavivattana, T. C. Wilson, V. Kersemans, S. Smart, M. Tredwell, B. G. Davis and V. Gouverneur, ^{18}F-Trifluoromethylation of Unmodified Peptides with 5-^{18}F-(Trifluoromethyl) dibenzothiophenium Trifluoromethanesulfonate, *J. Am. Chem. Soc.*, 2018, **140**, 1572–1575.

122 C. W. Kee, O. Tack, F. Guibbal, T. C. Wilson, P. G. Isenegger, M. Imiołek, S. Verhoog, M. Tilby, G. Boscutti, S. Ashworth, J. Chupin, R. Kashani, A. W. J. Poh, J. K. Sosabowski, S. Macholl, C. Plisson, B. Cornelissen, M. C. Willis, J. Passchier, B. G. Davis and V. Gouverneur, ^{18}F-Trifluoromethanesulfinate Enables Direct C–H ^{18}F-Trifluoromethylation of Native Aromatic Residues in Peptides, *J. Am. Chem. Soc.*, 2020, **142**, 1180–1185.

123 T. Günther, G. Tulipano, P. Dournaud, C. Bousquet, Z. Csaba, H.-J. Kreienkamp, A. Lupp, M. Korbonits, J. P. Castaño, H.-J. Wester, M. Culler, S. Melmed and S. Schulz, International Union of Basic and Clinical Pharmacology. CV. Somatostatin Receptors: Structure, Function, Ligands, and New Nomenclature, *Pharmacol. Rev.*, 2018, **70**, 763–835.

124 J. W. McDaniel, J. M. Stauber, E. A. Doud, A. M. Spokoyny and J. M. Murphy, An Organometallic Gold(III) Reagent for ^{18}F Labeling of Unprotected Peptides and Sugars in Aqueous Media, *Org. Lett.*, 2022, **24**, 5132–5136.

125 V. R. Bouvet and F. Wuest, Application of [18F]FDG in radiolabeling reactions using microfluidic technology, *Lab-on-a-Chip*, 2013, **13**, 4290.

126 S. Richter and F. Wuest, 18F-Labeled Peptides: The Future Is Bright, *Molecules*, 2014, **19**, 20536–20556.

127 D. J. Donnelly, J. Kim, T. Tran, P. M. Scola, D. Tenney, A. Pena, T. Petrone, Y. Zhang, K. M. Boy, M. A. Poss, E. L. Cole, M. G. Soars, B. M. Johnson, D. Cohen, D. Batalla, P. L. Chow, A. O. Shorts, S. Du, N. A. Meanwell and S. J. Bonacorsi, The discovery and evaluation of [18F]BMS-986229, a novel macrocyclic peptide PET radioligand for the measurement of PD-L1 expression and *in vivo* PD-L1 target engagement, *Eur. J. Nucl. Med. Mol. Imaging*, 2024, **51**, 978–990.

4894 | *Org. Chem. Front.*, 2025, **12**, 4871–4895

This journal is © the Partner Organisations 2025

128 S. Mukherjee, A. Rogers, G. Creech, C. Hang, A. Ramirez, M. Dummeldinger, S. Brueggemeier, C. Mapelli, S. Zaretsky, M. Huang, R. Black, M. B. Peddicord, N. Cuniere, J. Kempson, J. Pawluczyk, M. Allen, R. Parsons and C. Sfouggatakis, Process Development of a Macrocyclic Peptide Inhibitor of PD-L1, *J. Org. Chem.*, 2024, **89**, 6651–6663.

129 M. Badenhorst, A. D. Windhorst and W. Beaino, Navigating the landscape of PD-1/PD-L1 imaging tracers: from challenges to opportunities, *Front. Med.*, 2024, **11**, 1401515.

130 Y. Pan, The Dark Side of Fluorine, *ACS Med. Chem. Lett.*, 2019, **10**, 1016–1019.

This journal is © the Partner Organisations 2025

Org. Chem. Front., 2025, **12**, 4871–4895 | **4895**